GEOLOGICA CARPATHICA, JUNE 2019, 70, 3, 241–260 doi: 10.2478/geoca-2019-0014

The foreland state at the onset of the flexurally induced transgression: data from provenance analysis at the peripheral Carpathian Foredeep (Czech Republic)

SLAVOMÍR NEHYBA[1,✉], JIŘÍ OTAVA[2], PAVLA TOMANOVÁ PETROVÁ[2] and ADÉLA GAZDOVÁ[1]

[1]Department of Geological Sciences, Faculty of Science, Masaryk University, Kotlářská 2, 611 37 Brno, Czech Republic; ✉slavek@sci.muni.cz
[2]Czech Geological Survey, Leitnerova 22, 658 68 Brno, Czech Republic; jiri.otava@geology.cz, pavla.petrova@geology.cz

(Manuscript received October 25, 2018; accepted in revised form April 1, 2019)

Abstract: The Žerotice Formation recognised in a confined area NE–SE of Znojmo represents a basal member of the sedimentary succession of the southwestern margin of the Carpathian Foredeep in Moravia (Czech Republic). Two facies associations were recognised within the formation. The first one mantles the pre-Neogene basement with an irregular unconformity, reflects arid climatic conditions and deposition of episodic shallow, high-energy stream flows and/or mass flows (alluvial to fluvial deposits). The second facies association is interpreted as lagoonal to distal flood plain deposits. The barren unfossiliferous deposits of the Žerotice Formation are covered by nearshore marine Eggenburgian deposits. The boundary between these deposits represents a sequence boundary (i.e. the basal forebulge unconformity). Detailed provenance studies of successive beds below and above this sequence boundary showed differences in the source area and paleodrainage. Both the local primary crystalline rocks (Moravian and Moldanubian Unit, Thaya Batholith) and older sedimentary cover (especially Permo–Carboniferous sedimentary rocks) form the source of the Žerotice Formation. All these geological units are located only a few km away from the preserved areal extent of the deposits of the Žerotice Formation (short transport and a local source). The source areas of the overlying marine Eggenburgian beds are located far more to the W and NW in the Moldanubian and Moravian Units (longer transport, extended source area). Local confined preservation of the Žerotice Formation is preliminarily explained as connected with a tectonically predisposed paleovalley.

Keywords: Moravia, peripheral foreland basin, cratonward margin, paleovalley infill, basal forebulge unconformity, Egerian/Eggenburgian.

Introduction

Start of the deposition along the distal (i.e. "cratonward") margins of the peripheral foreland basins is generally strongly influenced by the local morphology of the foreland, itself partly controlled by former structural features of the bedrock. The paleovalleys entrenched into the bedrock are commonly preserved along basal unconformity surfaces (Baker 1984). Sedimentary infill of such paleovalleys provides unique information about the flexurally induced sea-level changes, the foreland paleodrainage network and the role of external factors (climate, tectonics, sediment supply and paleogeomorphology), supplies information about the geological situation bellow the foreland-basin succession and constitutes basic data for the stratigraphic organisation of sedimentary basins (Gupta 1999; Dalrymple 2004). The stratigraphic architecture of these valleys is determined by: a) the antecedent topography of the terrestrial valley system before inundation, and b) the rate of fluvial sediment influx vs. the rate of relative sea-level rise (Schumm & Etheridge 1994; Zaitlin et al. 1994; Gupta 1999).

The basal sedimentary cover of the southwestern margin of the Carpathian Foredeep (Alpine-Carpathian peripheral foreland basin) is deposited on a highly irregular erosional surface evolved in the crystalline rocks of the Bohemian Massif or its Paleozoic, Mesozoic and Paleogene sedimentary cover. Deep troughs/paleovalleys cut into the foreland are oriented mostly in a NW–SE direction almost perpendicularly to the main basin axis. Erosional troughs in partly similar position are also known from the Polish part of the Carpathian Foredeep (Oszczypko & Tomaś 1976; Jucha 1985; Oszczypko & Ślączka 1985; Karnkowski 1989; Połtowicz 1998; Karnkowski & Ozimkowski 2001; Oszczypko et al. 2006; Głuszyński & Aleksandrowski 2016), Ukraine (Shpak et al. 1999), from the North Alpine Foreland Basin (Kempf & Pfiffner 2004). Numerous fluvial incised valleys are also known from the southern margin of the Bohemian Massif in Austria, filled with e.g., St.Marein–Freischling Fm., Langau Fm., Freistadt Fm. of the Alpine–Carpathian Foredeep. Fluvial deposition in these paleovalleys started in Late Oligocene and was forced back during the Early Miocene transgression (Roetzel 2002).

An origin of the previously mentioned paleovalleys has been explained by early-Paleogene fluvial erosion of the uplifted Carpathian Foreland (Oszczypko & Tomaś 1976; Karnkowski 1989; Połtowicz 1998; Picha et al. 2006), partly or completely controlled structurally (Oszczypko & Ślączka 1985; Krzywiec 1997, 2001). These assumptions fit with the about 1.5 km deep Vranovice and Nesvačilka troughs filled with Paleogene

clastic deposits (Picha 1979; Picha et al. 2006). Newly the Žerotice trough was defined by Krejčí et al. 2017. According to Jarosiński et al. (2009) the fluvial incision of the Mesozoic and older strata of the Polish Carpathian Foreland occurred during late Oligocene to early Miocene and the incision only shortly or directly preceded the deposition of the flexurally induced transgression.

Deposits below and above the flexurally induced transgression within the paleovalleys are separated by "peripheral forebulge unconformity". The peripheral forebulge unconformity is a megasequence boundary separating the overlying foreland basin fills from the underlying passive margin sequences and differs from type 1 unconformity characterized by a major eustatic sea level fall (Crampton & Allen 1995).

Nehyba (2000) supposed the existence of a paleovalley cut into the foreland margin of the southwestern margin of the Carpathian Foredeep NE–SE of Znojmo (see Fig. 1). The deposits of the Žerotice Formation (Oligocene/Miocene), which represent the basal member of Neogene sedimentary succession of the southwestern margin of the Carpathian Foredeep were recognised within this paleovalley. The paper presented is focused on the sedimentary infill of the paleovalley with several goals: (i) to provide the sedimentological and provenance analysis of the Žerotice Fm.; (ii) to compare the provenance of successive beds of the foreland-basin infill below and above the flexurally induced transgressive surface/basal forebulge unconformity and (iii) to describe the paleodrainage evolution.

Geological setting

The southwestern margin of the Carpathian Foredeep, where the study area is located, represents a peripheral foreland basin formed due to the tectonic emplacement and crustal loading of the Alpine–Carpathian Thrust Wedge onto the passive margin of the Bohemian Massif (Nehyba & Šikula 2007; Fig. 1A). The stratigraphic range of the sedimentary infill of the Carpathian Foredeep is Oligocene/lower Miocene (Egerian) to middle Miocene (lower Badenian) (Brzobohatý & Cicha 1993; Fig. 2).

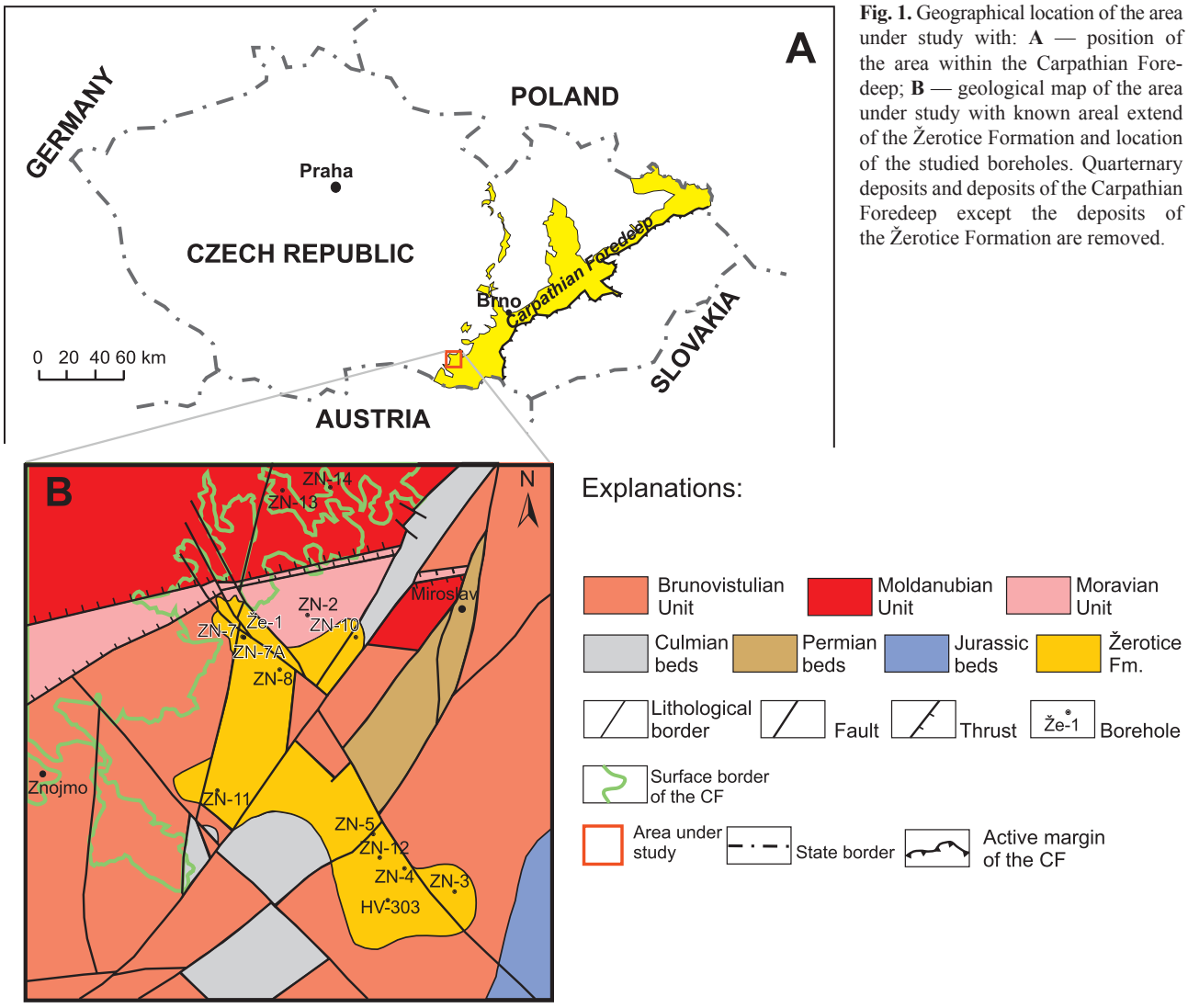

Fig. 1. Geographical location of the area under study with: **A** — position of the area within the Carpathian Foredeep; **B** — geological map of the area under study with known areal extend of the Žerotice Formation and location of the studied boreholes. Quarternary deposits and deposits of the Carpathian Foredeep except the deposits of the Žerotice Formation are removed.

Brunovistulian, Moldanubian and Moravian Units (Proterozoic–Paleozoic) create crystalline basement of the southern part of the Carpathian Foredeep. Culmian (Lower Carboniferous) sediments of the Moravosilesian Unit and Carboniferous–Permian sediments of the Boskovice Basin cover the crystalline fundament.

Whereas the Oligocene fluvial deposits of the St. Marein–Freischling Formation preceding the marine transgression of the Alpine Foredeep in Lower Austria are outcropped in numerous sections in a relative broad area (Nehyba & Roetzel 2010), the basal deposits of the Carpathian Foredeep in Moravia known as the Žerotice Member were recognised below the surface in a highly restricted area about 10 km NE–SE of Znojmo (Dlabač 1976; Čtyroký 1982, 1991). Originally Prachař (1970) described these deposits as Žerotice series according to the village nearby to borehole ZN-7, where they were firstly recognised. Later Dlabač (1976) used the term Žerotice Member and this term is still widely used (Brzobohatý 2002; Adámek 2003 etc.). However, from litostratigraphic point of view, these deposits should be designed of the Žerotice Formation (ŽFm) and this term is also used in this paper. Recently Roetzel (2017) reported sediments similar to the ŽFm at the margin of the Bohemian Massif in Austria and described them as the Ravelsbach Fm.

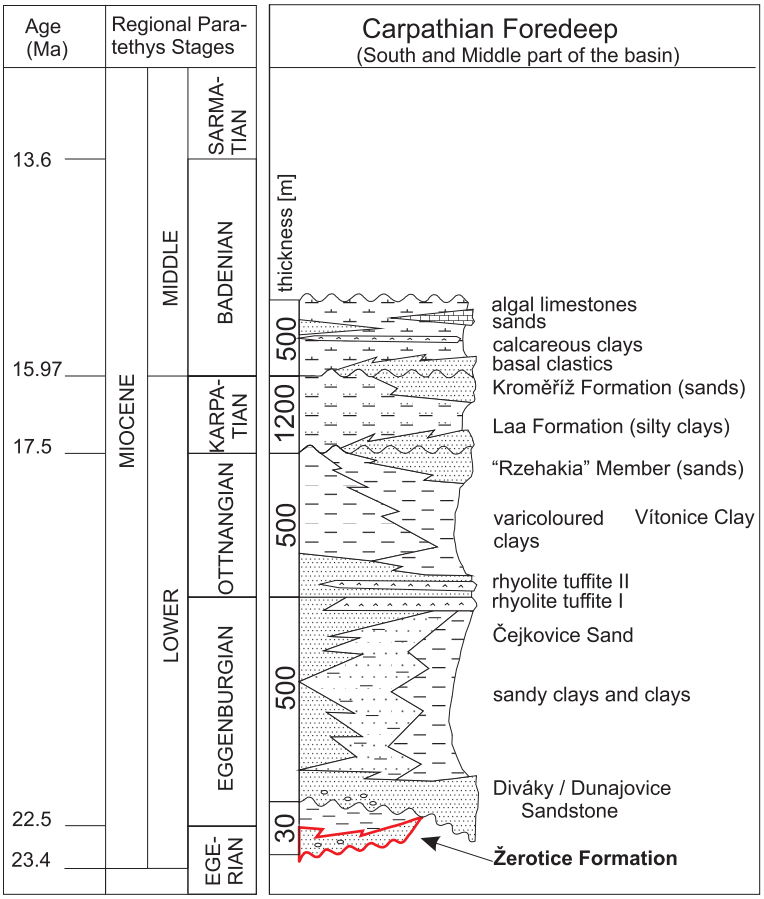

Fig. 2. Generalized stratigraphic scheme of the sedimentary infill of the southern and middle part of the Carpathian Foredeep with position of the Žerotice Formation (modified after Brzobohatý 2002, Adámek 2003 and Adámek et al. 2003).

The ŽFm forms a NW–SE prolonged narrow (about 2 km in width and about 15 km in length) belt localized between the village Žerotice and Božice (Krejčí et al. 2017). The actually known areal extent of the ŽFm is presented in Fig. 1B together with a schematized geological map of the area and boreholes under study (for position of the boreholes see Table 1).

Deposits of the ŽFm directly cover the crystalline basement or its Pre-Cenozoic sedimentary cover (Dlabač 1976; Čtyroký 1982). These variegated clays, silts, sands and gravels are barren of fossils and stratigraphically they are supposed to be Egerian(?) to Eggenburgian (Čtyroký 1982, 1991, 1993) or Oligocene (Dlabač 1976). Deposits of the ŽFm are overlain by shallow marine Eggenburgian beds and Čtyroký (1993) supposed a sedimentary transition between them. The deposits of the ŽFm were interpreted as deltaic or flash flood deposits under terrestrial conditions (Dlabač 1976). Čtyroký (1982) supposed that the ŽFm represents an alternation of depositions in shallow depression or lake sediments (green beds) and terrestrial flash floods sediments (red and violet beds). Interpretation of the ŽFm as terrestrial (alluvial, fluvial or lacustrine) beds can be followed in Krystková & Krystek (1981), Čtyroký (1991) and Brzobohatý & Cicha (1993).

The ŽFm is overlain by Eggenburgian, Ottnangian and finally lower Badenian deposits. Eggenburgian sediments are represented by diversified lithologies such as sands, siltstones and claystones (46 m in borehole Že-1, Čtyroký 1982). The spectrum of shallow water Eggenburgian sediments is characterised by basal gravels, sands and sandstones, often kaolinised, locally with numerous euhaline molluscs (e.g., *Glycymeris fichtelli*) or a brackish fauna (*Granulolabium moravicum*, *Crassostrea* sp.), and also clays and claystones with pieces of coal residues (Čtyroký 1982). A horizon of volcaniclastics has been recognized in this area and is correlated with the late Eggenburgian (Nehyba et al. 1999).

During Ottnangian the connection to the open sea was limited and Eggenburgian sediments were partly eroded during lower Ottnangian. Sands and clays with remains of fish and plants were deposited (Vítonice Clays) north of Znojmo. Volcaniclastic horizons are known in the early Ottnangian around Miroslav (Nehyba et al. 1999). A freshwater to brackish depositional environment, locally with an anoxic regime, was recognised during Ottnangian (Brzobohatý 2002).

Lower Badenian sediments that are represented by calcareous clays with typical foraminiferal fauna with *Orbulina suturalis* are preserved in a tectonically predisposed depression e.g. nearby Šatov (Roetzel et al. 2004).

Table 1: List of boreholes under study and their geographic coordinates (coordinate system WGS84).

Boreholes	Geographic coordinates	
	N	E
Že-1	48°55.4814	16°10.3320
ZN-2	48°53.0962	16°10.1938
ZN-3	48°49.5742	16°19.7166
ZN-4	48°50.0330	16°17.6581
ZN-5	48°50.8305	16°16.2531
ZN-7	48°55.4885	16°10.3415
ZN-7A	48°55.4858	16°10.3380
ZN-8	48°54.7603	16°11.9170
ZN-10	48°55.8003	16°14.7444
ZN-11	48°51.4763	16°10.0517
HV-303	48°49.1586	16°17.1272

Methods

The results of the study of deposits of the ŽFm and directly overlying Eggenburgian beds are based on the study of the preserved cores from boreholes ZN-4, ZN-5, ZN-7, ZN-8, ZN-12 and HV-303. Unfortunately, the cores are rare, discontinuous and volumetrically small because these boreholes were drilled more than five decades ago. Similarly, mostly only general descriptions of lithology and stratigraphy of sedimentary successions are available (Dlabač 1976). Such a situation limits the use of conventional methods of sedimentological analysis (Walker & James 1992; Tucker 1995; Collinson et al. 2006). Lithofacial analysis is therefore based mainly on primary description and textural data, because sedimentary structures were recognized rarely and mostly in preserved samples. Lithofacies were grouped into facies associations, i.e. assemblages of spatially and genetically related facies, which are also the expressions of different sedimentary environments.

Pebble petrography, shape and roundness were determined both in deposits of the ŽFm (4 samples) and in the overlying Eggenburgian beds (6 samples) within a grain-size fraction of larger than 4 mm. Shape and roundness were estimated under binocular microscope using the methods of Zingg (1935) and Powers (1982).

Combined sieving and laser methods were used for grain size analysis (12 analyses). The coarser grain fraction (4–0.063 mm, wet sieving) was analysed by a Retch AS 200 sieving machine and a Cilas 1064 laser diffraction granulometer was used for the analyses of the finer fraction (0.4 μm–0.5 mm). Ultrasonic dispersion, distillate water and washing in sodium polyphosphate were used prior to analyses in order to avoid flocculation of the particles analysed. The average grain size is illustrated by the graphic mean (Mz) and the uniformity of the grain size distribution/sorting by the standard deviation (σ_I) (Folk & Ward 1957).

The gamma-ray spectra (GRS) was measured by a GR-320 enviSPEC laboratory spectrometer with a 3×3 in. NaI(Tl) scintillation detector (Exploranium, Canada). Counts per second in selected energy windows were directly converted to concentrations of K (%), U (ppm) and Th (ppm). One measurement of 30 minutes was performed for each sample measured (19 samples from the ŽFm and 7 samples from Eggenburgian beds — min. 300 g). The total radioactivity i.e. "standard gamma ray" labeled as SGR was estimated from the following relationship: SGR [API]=16.32×K (%)+8.09×U (ppm)+3.93×Th (ppm) (API units/American Petroleum Institute units) (Rider 1996).

Heavy minerals were studied in 9 samples from 5 boreholes in the grain size fraction 0.063–0.125 mm. The chemistry of garnet was analysed in 87 grains, the chemistry of both rutile and tourmaline was based on data from 21 grains each. Electron microprobe analysis was done on a CAMECA SX 100 electron microprobe analyser in the Laboratory of Electron Microscopy and Microanalysis of the Faculty of Science, Masaryk University, Brno. Measurements were carried out under following conditions: wave propagation mode, accelerating voltage 15 keV, beam current 10 nA (tourmaline) and 20 nA (garnet, rutile), beam size 5 μm (tourmaline) and 2 μm (garnet, rutile). Zircon studies (external morphology, colour, presence of older cores, inclusions and zoning, elongation) were carried out on 255 grains from 3 samples from 3 boreholes (grain size fraction 63–125 μm). Results of zircon typology are based on 55 crystals.

For a purpose of micropaleontological studies, 8 samples from 4 boreholes, were used. Sediments were soaked in warm water with sodium carbonate for disaggregation, and then washed under running water through 63 μm mesh sieves. Microfauna was picked from the fraction, and identified with a NIKON SMZ 745T binocular microscope. Occurrence of foraminiferal assemblages indicating biostratigraphy and paleoecology of sediments was supposed.

Results

Facies analysis

Sedimentological study of the succession led to the distinction of 13 lithofacies. Descriptions and interpretations of these lithofacies are given in Table 2. These descriptions and interpretations are a little vague due to poor primary description and the very limited number of samples for revision. Three facies associations (FA) have been identified within the studied sedimentary succession. The distribution of lithofacies and facies associations in selected boreholes is presented in Fig. 3. Deposits of FA 1 and FA 2 represent the ŽFm and FA 3 comprise the overlying Eggenburgian deposits.

The first facies association (FA 1) mantles the pre-Neogene basement with an irregular unconformity surface and is overlaid by deposits of FA 2. FA 1 is composed of lithofacies M1, S1, S3, G1 and G2. FA1 is formed mostly (47.0 %) by very thick bedded (1–4 m thick) massive mudstones of facies M1. Medium to very thick bedded (0.2–3 m) massive sandstones of facies S1 are also common (23.0 %) similarly to the medium to very thick bedded poorly sorted coarse grained sandstones

Table 2: Descriptive summary list of lithofacies of the studied deposits distinguished in the cores or based on primary description of the boreholes. The graphic mean Mz and the standard deviation σ_I were calculated after Folk & Ward (1957).

Symbol	Description	Interpretation
M1	Greyish green, light brown, olive brown, yellowish green, light green reddish or blue green mottled "variegated" mudstone (siltstone, silty clay to claystone). Mostly massive, common tectonic deformations (fractures, fault polish). Admixture of sand and of small pebbles (mostly subangular, less commonly rounded) of whitish quartz, gneisses, limestones, shales). Faint lamination very rare. Mz=0.03–0.07 mm, σ_I=1.8–2.0 ϕ	Suspension deposits, admixture of material transported by traction. Fine-grained floodplain deposits to lagoonal deposits.
M2	Greyish brown, dark grey mudstone (clay to claystone, clayey siltstone), massive, rich in content of coalified plant detritus or coal fragments.	Estuarine–lagoon suspension deposits.
M3	Greenish grey, both light and dark grey mudstone (clayey silt to silty clay) with common occurrence of shells or shell debris. Planar parallel laminated (mostly horizontal, less commonly undulated). Rhythmic alternations of laminas rich and poor in content of shell debris (Mollusca) recognised rarely.	Estuarine to marine–transition zone.
S1	Green grey, grey green, light green, sometime reddish mottled, fine, fine to medium sandstone. Mostly relatively well sorted, less commonly admixture of gravelite (clast up to 5 mm in diameter). Massive, admixture of white mica, rare fragments of coalified plant detritus. Mz=0.13–0.27 mm, σ_I=1.9–2.8 ϕ	Fluvial bars to delta mouth bars.
S2	Whitish grey, yellowish grey medium to coarse grained sandstone. Well sorted. Mostly calcareous.	Nearshore deposits.
S3	Grey to dark grey, dark green grey, olive green, medium, medium to coarse or very coarse grained sandstone sometimes with admixture of subangular clasts up to 1 cm in diameter. Massive, matrix rich in clay. Mz=0.18 mm, σ_I=2.2 ϕ	Storm washover or fluvial flood flow deposits.
S4	Grey, beige brown, very fine sandstone to siltstone, plane parallel lamination or ripple lamination. Sometimes alternations of silty and sandy laminas. Common occurrence of shell debris, significant content of light mica. Mz=0.14 mm, σ_I=2.9 ϕ	Nearshore deposits.
S5	Grey, dark grey fine to medium grained sand to sandstone, relative well sorted, laminated, calcareous. Higher content of shell detritus (Mollusca, Ostrea,..), rich in coalified plant detritus.	Nearshore deposits.
G1	Green grey, dark green, reddish mottled pebbly mudstone. Subrounded to subangular pebbles of crystalline rocks (up to 3 cm in diameter) scattered in claystone. Intraclasts of darker claystones are less common. Sometime fractured and deformed. Mz=0.28 mm, σ_I=2.9 ϕ	Deposits of mass flows (cohesive debris flows).
G2	Grey sandy gravel to conglomerate. Clast to matrix supported, massive. Subrounded pebbles up to 5 cm in diameter (mostly about 2 cm). Pebbles are formed by quartz, quartzite, granitoids. Poorly sorted coarse to very coarse sandstone matrix.	Mass flows (noncohesive debris flows), stream flows (flood flows).
Fe	Green grey to yellow brown oolitic ironstone. Diameter of oolites of about 1 mm.	Protected coastal settings or lagoon.
T	Tectonic breccia — angular fragments of claystone and sandstone.	Postdepositional deformation of M1 or M2 facies.

of facies S3 (21.2 %). Poorly sorted pebbly mudstones of facies G 1 (7.4 %) and massive clast- or matrix-supported pebbly conglomerates of facies G2 (1.4 %) are less common. The thickness of FA 1 is difficult to estimate, because its base was often not reached by the drillings. The facies succession mostly displays a fining upward trend, together with an upward decrease of maximum grain size.

The second facies association FA 2 is composed by of lithofacies M1, M2, S1, S3, G1, Fe and T. Thick to very thick bedded (0.4–8m thick) massive mudstones of facies M1 form the predominant part of FA 2 (59.1 %). Medium to very thick bedded massive sandstones of facies S1 form 22.2 % and poorly sorted coarse grained sandstones of facies S3 comprise 12 %. Occurrences of the rest of the facies are very low (T — 1.0 %, G1 — 0.4 %, M2 — 0.2 % and Fe — 0.2 %). FA2 either overlies the deposits of FA1 or directly covers the bedrock. FA2 is overlaid by the deposits of FA3 with a sharp contact. Ferriferous oxides and hydroxides are a significant part of the residuum. From a micropaleontological point of view, the residua are barren of foraminifers. Some fragments of unidentifiable tests of gastropoda and bivalvia and fragments of teleostei bones and vertebra were found. The recognized thickness of deposits of FA1+2 (i.e. the ŽFm) varies highly between 4.5 and 65 m. The higher thicknesses were generally recognised towards NW.

The third facies association FA 3 is composed of lithofacies M2, M3, S1, S2, S4 and S5, and represents the uppermost part of the succession studied. Laminated fossiliferous mudstones of facies M3, laminated or rippled very fine sandstones of facies S4 and S5 prevail in the studied part of FA3. Deposits of FA3 are typically calcareous with characteristic occurrence of mollusc shells or their detritus. Only the lower most portion of the sedimentary pile of FA 3 was evaluated. Sediments contain relatively abundant fragments of mollusc tests (gastropoda and bivalvia), rarely fragments of bones, scales, tooth and vertebra of teleostei. Tests are damaged and wrinkled.

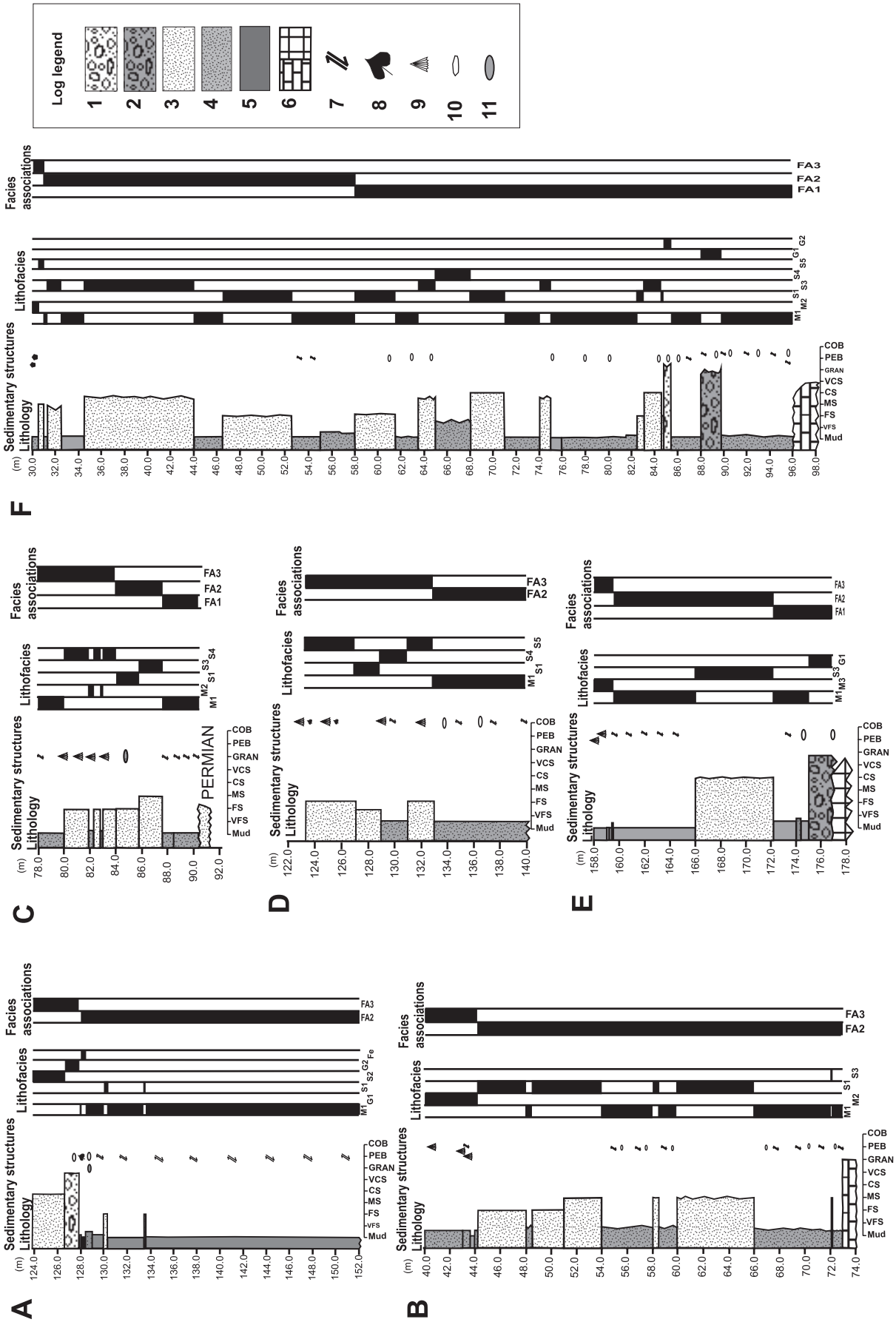

Fig. 3. Sedimentological core logs of the boreholes: **A** — borehole ZN-4; **B** — borehole ZN-8; **C** — borehole ZN-5; **D** — borehole ZN-12; **E** — borehole HV-303; **F** — borehole ZN-7, with lithofacies and facies associations. Log legend: 1 — gravel; 2 — pebbly mudstone; 3 — sand; 4 — sandy mud, silt; 5 — clayey mud, clay; 6 — Paleozoic/crystalline basement; 7 — tectonic deformation, fissures; 8 — plant fragments; 9 — shells; 10 — outsized pebbles, cobbles; 11 — mudstone intraclasts.

Interpretation: The dominant thick bedded arrangement of FA 1, poorly organized texture, evidence of clast- to matrix-supported conglomerates and a general lack of stratification point to a non-selective, en-masse style of deposition partly (conglomeratic facies) from flows of high sediment concentration (Nemec & Steel 1984; Went 2005). Conglomeratic facies are attributed to cohesive- and non-cohesive sediment debris flows (Lowe 1982) or debris flows and hyperconcentrated density flows (Mulder & Alexander 2001). However, the predominant massive mudstones of facies M1 reveal relatively quiet depositional conditions with suspension deposition (standing-water floodbasin). Alternation of deposits of M1 with sandstone lithofacies S1, S3, which are interpreted as traction deposits and conglomerates G1, G2 signalize dramatic changes in the transportation agents and deposition. Such a situation is common in relatively arid climatic conditions with episodic shallow, high-energy stream flows or mass flows (Hampton & Horton 2007). The poor sorting is connected with flashy discharge. Alternation of more or less humid/arid conditions could be signalized by the variegated colour of deposits. However, it could be also a signal of erosion of lateritic crusts. Deposits of FA 1 are therefore interpreted as alluvial to fluvial deposits. Deposition of facies M1 might have occurred during recessional flood stages or during the long intervals between major flash floods (Blair 1999) and represents a flood plain (Bridge & Demicco 2008). The fining-upward arrangement of FA 1 is interpreted as evidence of a decrease in transporting capacity and discharge of the flows filling the negative relief/valley and by infill aggradation (Lewin & Ashworth 2014). It might be an evidence of discharge variations and water ponding that controlled the alternation between flooding, stagnation and infiltration (Marconato et al. 2014). Another possibility is a terminal fan/fluvial distributary system (Nichols & Fischer 2007), which developed under the influence of semi-arid to arid climatic regimes. Multiple small and shallow distributive channels co-exist in such fan-like depositional systems, leading to rapid shifting from an active to an abandoned tracts/part of the system (Weissmann et al. 2010). The fining upward arrangement might also be connected with the retrograding character of a depositional system (i.e. cratonward retreat).

Deposits of FA 2 were interpreted as distal flood plain/flood basin deposits influenced by water flows (Mertz & Hubert 1990). Variegated colour and mottling might signalize subaerial exposure and/or erosion of lateritic crusts. Occurrence of coalified plant detritus, dominance of planar lamination, and rhythmic alternation of mudstone and sandstone facies point to alternation of deposition from suspension and traction, and the common low relief of the depositional plane. Continued fluvial influence and sediment support is indicated by the presence of thin flood-generated interbeds or thicker beds of facies S1 or S3 (washover beds, crevasse-splay lobes, mouth bars or a possible bayhead delta) within dominant mudstones of facies M1 (standing-water conditions in floodbasins; Fralick & Zaniewski 2012). Plant fragments reveal humid conditions with a positive hydrological budget in the source area and rapid deposition (e.g., Fielding 1985; Fernández et al. 1988; Lottes & Ziegler 1994).

Relatively good sorting (comparing to deposits of FA1+2) of deposits of FA 3, the common clean texture of both sandy and muddy facies suggest reworking by wave and/or tide action in a nearshore environment, which is consistent with the occurrence of fragments of unidentifiable tests of fossil molluscs–gastropoda and bivalvia. A relatively proximal marine realm can be inferred from the important role of sandstones and content of mollusc shells. The occurrence of terrestrial organic matter debris suggests fluvial/deltaic support nearby or coastal flats (Dietrich et al. 2017). Deposits of FA 3 are therefore interpreted as nearshore deposits connected with Eggenburgian marine transgression. They are equivalent to the marginal shallow marine development of Eggenburgian deposits of Čtyroký (1982, 1991). The flexurally induced transgressive surface is located along the base of FA3.

Provenance analysis

Provenance analysis is based on the pebble petrography and analysis of heavy minerals.

Petrography and size of pebbles, shape and roundness of pebbles

The composition of granules and pebbles within deposits of the ŽFm varies. Quartz pebbles dominate in the majority of samples forming 20–100 % of the pebble spectra. Varieties of quartz are present. Whitish, milky quartz is the main type, with dark or light grey, brown and pinkish types subordinating. Crystalline metamorphic rocks form an important part of the pebble and granule suite with a dominance of phyllites (up to 40 %) and mica schists (up to 10 %). Quartzite, greenschist and quartz+feldspar aggregate were recognised exceptionally. Sandstones (brown or reddish fine or coarse grained quartzose ones) were identified in some samples, forming up to 25 % of the spectra. Pebbles and granules reveal a mostly (44 %) bladed shape. Discs were less common (28.8 %), similarly to spheres (17 %) or rods (10.2 %). Clasts were mostly angular (70.4 %) followed by subangular ones (23.6 %). Subrounded (5.5 %) or even rounded (0.5 %) clasts are significantly less common.

The composition of granules and pebbles of the overlying Eggenburgian beds (FA 3) is remarkably simpler. Quartz content highly varies, forming up to 100 % in one sample and missing in other ones. Clastic sedimentary rocks play a dominant role in pebble and granule spectra. They are represented by light grey siltstone (up to 100 %), fine to coarse grained quartzose sandstone (up to 54.3 %), and calcareous fossil rich sandstone (up to 28.6 %). Pebbles of crystalline rocks were not recognised. Clasts reveal mostly (50.8 %) a disc shape. Blades were also common (41 %) to the expense of spheres (4.5 %) and rods (3.7 %). Clasts are mostly angular (49.4 %) or subangular (36.6 %); however, the content of subrounded (11.2 %) and rounded (3.0 %) clasts is higher than in deposits of the ŽFm.

Heavy minerals

Heavy minerals are sensitive indicators of provenance, weathering, transport, deposition and diagenesis (Morton & Hallsworth 1994), especially if combined with the chemistry of selected heavy minerals (Morton 1984). The ZTR (zircon+tourmaline+rutile) index is widely accepted as a criterion for the mineralogical "maturity" of heavy mineral assemblages (Hubert 1962; Morton & Hallsworth 1994) in the case of derivation from a similar source. Garnet, rutile, zircon and tourmaline are relatively stable in diagenesis and have a wide compositional range. Therefore, they enabled a detailed evaluation of the deposits studied.

Heavy mineral assemblages

The heavy mineral assemblages of the ŽFm highly varied. Whereas garnet (13.3–49.9 %) and also rutile (30–34.8 %) were common in all samples studied, the content of zircon (4.8–24.1 %), kyanite (0.2–22.4 %) and apatite (1.8–20 %) significantly varied in individual samples. The other heavy minerals i.e. staurolite, tourmaline, monazite, epidote, apatite, titanite, spinel, andalusite, and sillimanite are accessory, forming only a few percent each. The value of ZTR ranges between 17.8 and 60.8 %.

The heavy mineral spectra of the overlying Eggenburgian beds is significantly simpler with a typical garnet (49–53 %)–staurolite (25–39 %) assemblage. The other heavy minerals such as amphibole, epidote, kyanite, tourmaline, zircon, apatite, rutile, sillimanite, titanite, andalusite, monazite, anatase and brookite are accessory, forming only a few percent each. The value of ZTR was always below 10 %.

The heavy mineral spectra of the underlying Permian beds include in various ratios garnet, rutile, and apatite and less commonly (under 10 mod. %) also zircone. Such assemblages are generally common in Permian sediments in close vicinity.

Composition of garnet

The chemistry of detrital garnet is widely used for the more detailed determination of source rocks (Morton 1984). Ten garnet types were recognised for the deposits of the ŽFm and eight garnet types were identified within the overlying Eggenburgian beds (see Table 3). It is evident that although the garnet types are similar (with the strong dominance of almandines), differences in the garnet spectra of these two stratigraphic units exist.

Several ternary discrimination diagrams were utilized for more detailed identification of the primary source of garnet (Fig. 4). The PRP–ALM+SPS–GRS diagram (Mange & Morton 2007) in Figure 4A reflects the dominant source of garnets for rocks of the ŽFm from amphibolite-facies metasedimentary rocks or intermediate to felsic igneous rocks (both 30 %). Significantly less common are garnets from high-grade mafic rocks (15 %) and high-grade granulite-facies metasediments and intermediate felsitic igneous rocks (12.5 %). Garnets from ultramafics like pyroxenites and peridotites (7.5 %) or metasomatic rocks, and very low-grade metamafic rocks (5 %) are rare. The overlying marine Eggenburgian beds reveal a dominant (31.4 %) source from amphibolite-facies metasedimentary rocks and high-grade granulite-facies metasediments or intermediate felsitic igneous rocks (28.6 %). Garnets from intermediate to felsic igneous rocks (20 %) and garnets from high-grade mafic rocks (17.1 %) are less common. Garnets from ultramafics (2.9 %) are rare.

The PRP–ALM–GRS diagram (Méres 2008; Aubrecht et al. 2009) in Figure 4B indicates the dominant (56.1 %) primary source of garnets for the rocks of the ŽFm, derived from amphibolite-facies rocks, serpentinites and igneous rocks. Less common (22 %) are garnets from higher amphibolite- to granulite-facies rocks and also garnets from eclogite- and granulite-facies rocks (14.6 %). Garnets from high- to ultrahigh-pressure rocks are rare (7.3 %). The overlying Eggenburgian rocks reveal a dominant source from amphibolite facies rocks, serpentinites and igneous rocks (47.1 %) and from eclogite- and granulite-facies rocks (32.4 %). Less common (17.6 %) are garnets from higher amphibolite- to granulite-facies rocks and exceptional (2.9 %) are garnets from high- to ultrahigh-pressure rocks.

Diagram GRS–SPS–PRP (Fig. 4C) enables a comparisson to the potential source rocks of the eastern margin of the Bohemian Massif (Otava et al. 2000; Čopjaková et al.

Table 3: Recognised garnet types in the deposits of the Žerotice Formation, the overlying Eggenburgian beds and also Permo–Carboniferous beds of the Boskovice Basin (data from Nehyba et al. 2012).

Garnet type	Žerotice Fm.	Eggenburgian beds	Boskovice Basin
$ALM_{50–80}PRP_{11–47}GRS_{1–7}SPS_{1–7}ADR_{0–2}$	34.9 %	35.3 %	50.4 %
$ALM_{58–74}GRS_{10–23}PRP_{4–9}SPS_{2–8}ADR_{3–4}$	16.3 %	23.5 %	16.7 %
$ALM_{73–77}SPS_{16–17}PRP_{4–6}GRS_{0–2}ADR_{0–2}$	–	8.8 %	4.5 %
$ALM_{80–90}$ $PRP_{4–10}$ $SPS_{2–8}GRS_{0–8}$ $ADR_{0–2}$	7.0 %	5.9 %	5.3 %
$ALM_{47–57}SPS25_{–28}Prp_{3–11}$ $GRS_{10–11}$ $ADR_{3–4}$	2.3 %	–	3.9 %
$ALM_{42–62}GRS_{19–28}PRP_{14–27}SPS_{1–2}ADR_{0–2}$	7 %	8.8 %	11.3 %
$ALM_{55–75}PRP_{12–33}GRS_{11–28}SPS_{1–8}$ $ADR_{1–3}$	16.3 %	11.8 %	2.3 %
$ALM_{54–57}GRS_{21–25}SPS_{13–16}PRP_{4}$ $ADR_{1–4}$	2.3 %	2.9 %	0.8 %
$PRP_{68–73}ALM_{16–17}GRS_{0–6}SPS_{1–2}ADR_{3–4}UVA_{0–10}$	7.0 %	2.9 %	–
$PRP_{42}ALM_{35}$ $GRS_{20}ADR_{2}SPS_{1}$	2.3 %	–	–
$GRS_{56–65}ADR_{24–33}$ $ALM_{7}SPS_{1–2}PRP_{1}$	4.7 %	–	1.5 %
$ALM_{(69)}–PRP_{(18)}–SPS_{(12)}$	–	–	0.8 %
$GRS_{(74)}–PRP_{(13)}–ADR_{(12)}$	–	–	0.8 %
$GRS_{(50)}–ALM_{(41)}$	–	–	0.8 %
$PRP_{(40)}–ADR_{(36)}–ALM_{(20)}$	–	–	0.8 %

2002; Buriánek et al. 2012). A significant part of the garnets of the ŽFm might originate from the Moravian Unit (27.8 %), Moravian–Silesian Paleozoic/Culmian rocks (35.2 %) or from the Moldanubian Unit (14.8 %). The source of garnets from the Eggenburgian rocks is located in the Moravian Unit (41.2 %) and Moravian–Silesian Paleozoic/Culmian rocks (41.8 %).

Remarkable similarities can be recognized between garnets from the ŽFm and garnet spectra from the Permo–Carboniferous beds (Nehyba et al. 2012; Nehyba & Roetzel 2015) of the Boskovice Basin (see Table 3).

Composition of rutile

Rutile as an ultrastable mineral is commonly used for the provenance studies (Force 1980; Zack et al. 2004a,b; Triebold et al. 2007).

The concentrations of the main diagnostic elements (Fe, Nb, Cr and Zr) vary significantly in the ŽFm samples. The content of Fe shows that 41.7 % of l rutiles evaluated originated from magmatic rocks (pegmatites) and 58.3 % from metamorphic rocks. The concentration of Nb ranges between 420 and 12130 (average/AVG 2781 ppm), the concentration of Cr varies between 60 and 5540 ppm (AVG 1728 ppm), the concentration of Zr ranges between 100 and 1490 ppm (AVG 611 ppm) and most (75 %) of log Cr/Nb values are negative. A discrimination plot of Cr vs. Nb is shown in Figure 5 and reveals that the majority (50 %) of metamorphic rutiles originate from metapelites (mica-schists, paragneisses, felsitic granulites), and slightly more than one third (37.5 %) originate from metamafic rocks (eclogites, basic granulites), according to the grouping by Zack et al. (2004a,b) or Triebold et al. (2007). According to the diagnostic criteria of Triebold et al. (2012) all metamorphic rutiles originate from metapelites. The results of Zr-in-rutile thermometry (applied to metapelitic rutiles only — see Zack et al. 2004a,b; Meinhold et al. 2008) indicate that

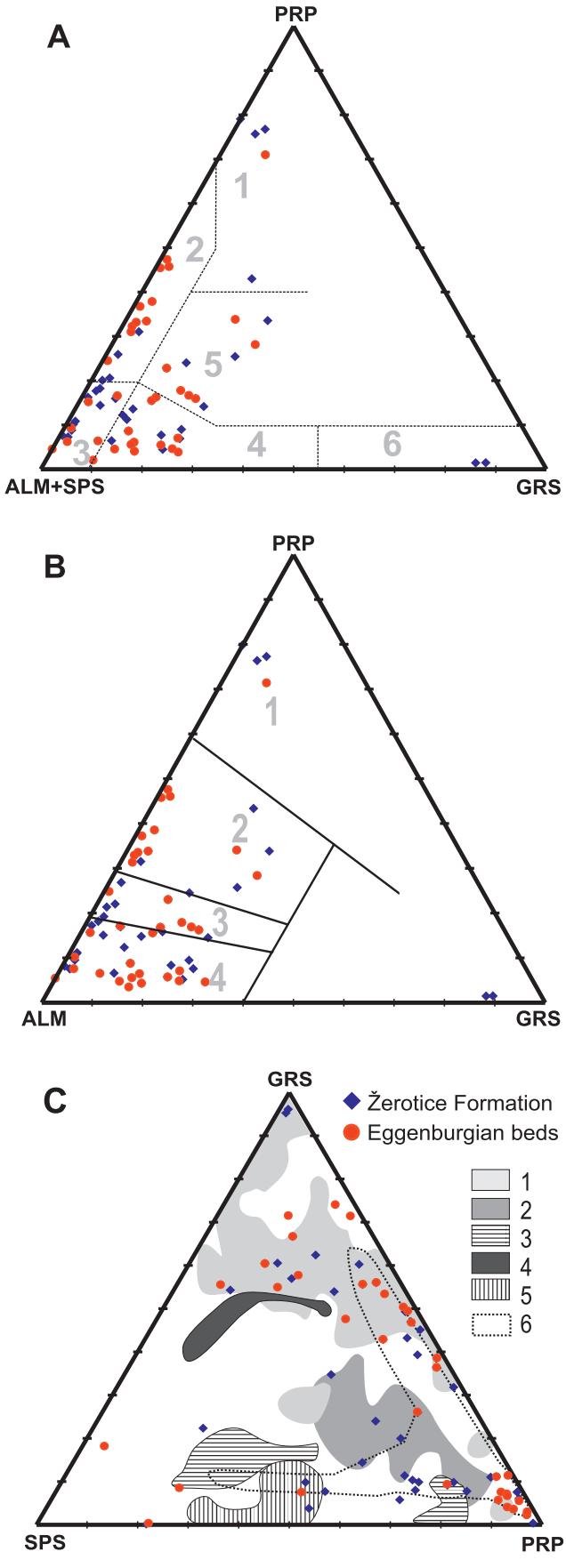

Fig. 4. Ternary diagrams of the chemistry of detrital garnets (ALM — almandine, GRS — grossular, PRP — pyrope, SPS — spessartine): **A** — discrimination diagram according to Mange & Morton (2007) (1 — pyroxenes and peridotites, 2 — high-grade granulite-facies metasediments and intermediate felsic igneous rocks, 3 — intermediate to felsic igneous rocks, 4 — amphibolite-facies metasdimentary rocks, 5 — high-grade mafic rocks, 6 — metasomatic rocks, very low-grade metamafic rocks and ultrahigh temperature metamorphosed calc–silicate granulites); **B** — discrimination diagram according to Méres (2008), Aubrecht et al. (2009) (1 — pyroxenes and peridotites, 2 — felsic and intermediate granulites, 3 — gneisses and amphibolites metamorphosed under pressure and temperature conditions transitional to granulite and amphibolite facies metamorphism, 4 — gneisses metamorphosed under amphibolite facies conditions); **C** — Ternary diagram of the chemistry of detrital garnets in comparison with possible source areas (1 — Moravian Unit, 2 — Moldanubian Unit, 3 — Svratka Crystalline Complex, 4 — granites of the Brno Massif, 5 — migmatites of the Brno Massif, 6 — younger part of the Moravian–Silesian Paleozoic/Culmian). Data from source rocks according to Otava et al. (2000); Čopjaková et al. (2002, 2005) and Buriánek et al. (2012).

rutiles originated from highly metamorphosed crystalline rocks (granulite, amphibolite and eclogite facies).

The concentrations of the main diagnostic elements (Fe, Nb, Cr and Zr) also vary significantly in the samples from Eggenburgian deposits. The content of Fe shows that 22.2 % of rutiles originate from magmatic rocks (pegmatites) and 87.8 % from metamorphic rocks. The concentration of Nb ranges between 640 and 15990 ppm (AVG 3580 ppm), the concentrations of Cr ranges between 100 and 4080 ppm (AVG 1204 ppm), the concentration of Zr varies between 100 and 8800 ppm (AVG 2100 ppm) and most (88.9 %) of log Cr/Nb values are negative. The discrimination plot of Cr vs. Nb (Fig. 5) reveals that the metamorphic rocks mostly originate from metapelites (75 %) and the source from metamafic rocks is less common (25 %) (Zack et al. 2004a, b; Meinhold et al. 2008; Triebold et al. 2012). According to the diagnostic criteria of Triebold et al. (2012) all metamorphic rutiles originated from metapelites. The application of "Zr-in-rutile thermometry" in metapelitic rutiles (Zack et al. 2004a, b; Meinhold et al. 2008) points to broad spectra of metamorphic rocks (green schists, amphibolite-, granulite-, eclogite-facies).

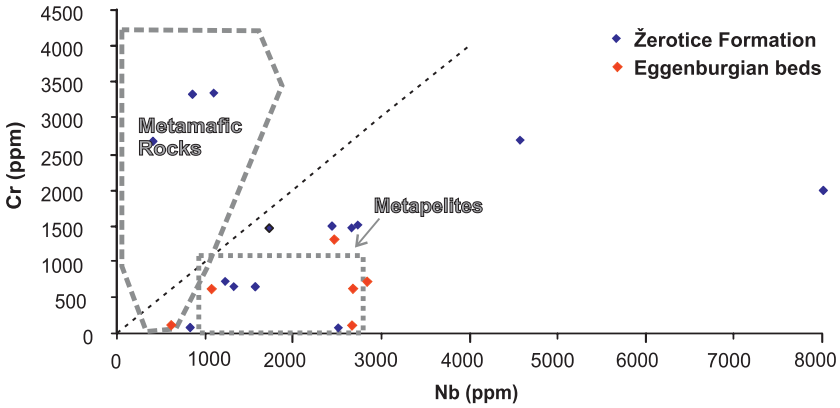

Fig. 5. Discrimination plot Cr vs. Nb of investigated rutiles (after Zack et al. 2004b).

Zircon studies

Zircon as very stable mineral is used for evaluation of the source rock, the role of recycling and the erosion rate (Poldervaart 1950; Mader 1980; Winter 1981; Lihou & Mange-Rajetzky 1996). Zircons were evaluated only for the ŽFm.

Euhedral zircons represent 4.3 to 11.8 %, subhedral zircons form 25.9 to 32.4 % and rounded to subrounded ones 55.9 % to 67.6 % of the zircon spectra. Crystal faces were identified at 52.7 to 78.1 % zircon grains. Fracturing of zircon grains were relatively common (33.6 % to 49.1 % of the grain spectra). Grains fractured nearly parallel to the c-axis were more common (28.3 to 41.8 %) than grains fractured perpendicular to the c-axis (5.3 to 7.3 %). Cracks were recognised in the majority of grains (72.7 to 96.9 %). The high portion of broken zircons points to primarily higher content of zircons with high value of elongation. Colourless zircons form 23.5 % to 41.1 %, zircons with a pale colour 49.1 to 60.9 %, brown ones 3.1 to 3.3 % and pink zircons 0 to 1.8 %. The proportion of zoned zircons was relatively low (10 to 21.9 %), zircons with older cores were rare (0.9 to 8 %). Inclusions were recognised in 79.1 to 93.8 % of the grains studied.

Elongation (the relationship between the length and width of crystals) was used as an indicator for possible host rocks, cooling rate and transport duration (Poldervaart 1950; Hoppe 1966; Zimmerle 1979; Finger & Haunschmid 1988). The average value of elongation of the zircons studied is 2.05 and the distribution of elongation is shown in Figure 6A. Zircons with elongation <2.0 are more common (60.4 %) than zircons with elongation >2.0 (39.6 %). Zircons with an elongation of >3 represent 6.3 %. Such zircons are supposed to reflect a volcanic origin and/or limited transport (Zimmerle 1979). The maximum elongation was 6.75; however, broken prisms of columnar crystals of zircon were relatively common.

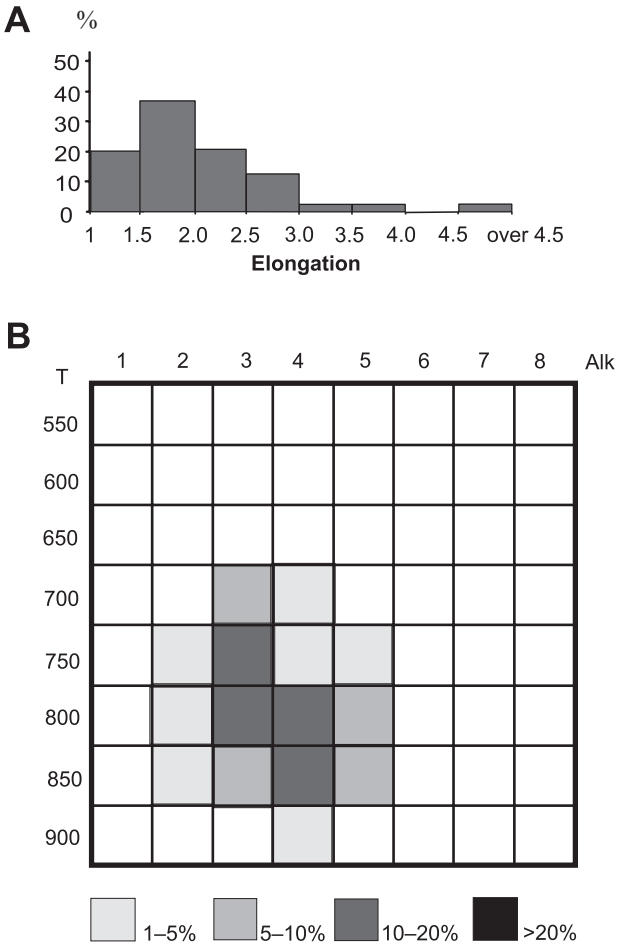

Fig. 6. Diagrams for studied zircons. **A** — Histogram of zircon elongation; **B** — typology of the zircons in the Pupin diagram (Pupin 1980).

Evaluation of zircon typology according to Pupin (1980, 1985) is based on the external zircon faces (both pyramids and prisms). This method assumes that the parent magma (especially the aluminium and alkali content and the crystallisation temperature) show a correlation with the produced zircon subtype. A standard designation was proposed for 64 zircon subtypes (Pupin 1980, 1985). In the case studied, a relatively broad spectrum of subtypes has been recognised. The most common were the typological subtypes S12 (17.9 %), S17 (14.5 %), S23 (11.6 %) and S18 (10.2 %). Further subtypes i.e. S7, S19, S22, S13, S24, S16, S8, S21, S14, S11 and J3 were less common. The distribution and abundance of zircon subtypes in the typological diagram of Pupin (1980) are shown in Figure 6B. The diagram shows a slightly higher occurrence of crystals with flat [101] pyramids over steep ones [211] and a predominance of the prism form [100] over the form [110] and points to the hybrid character of the parent magma.

Tourmaline

Generally, tourmaline chemistry of the analysed grains from the ŽFm and Eggenburgian beds range to a moderate degree in major and minor element concentrations — SiO_2: 34.3–36.3 %, Al_2O_3: 28.1–34.5 %, FeO: 5.2–12.0 %, MgO: 1.9–8.3 %, CaO: 0.1–2.1 %, Na_2O: 1.2–2.5 %, TiO_2: 0.4–2.3 %, F: 0.1–0.6 %, K_2O: 0–0.1 % and MnO: 0–0.3 %. Analyzed tourmalines represent mixtures of dravite and schorl (Fig. 7). Tourmalines of the ŽFm are slightly more commonly dravites (66.7 %) than shorls (33.3 %), similarly to the tourmalines of Eggenburgian beds (dravites 53.8 % and schorls 46.2 %).

Several ternary discrimination diagrams were utilized for more detailed identification of the primary source of tourmaline (Fig. 8). The Al–Fe+Mn–Mg and Fe–Mg–Ca diagrams (after Henry & Guidotti 1985) in Figure 8A and 8B indicate the source of tourmaline of both the ŽFm and marine Eggenburgian beds to be mostly from metapelites and metapsamites and also from Li-poor granitoids. Provenance-discrimination plots of Al–Fe+Mn–Mg and VAC–Na–Ca (data from possible source rocks after Buriánek et al. 2012) reveal a generally mixed source from both the Moravian Unit (ŽFm 62.5 %, Eggenburgian beds 70 %) and the Moldanubian Unit (ŽFm 37.5 %, Eggenburgian beds 40 %) (Fig. 8C,D). In general, no significant differences were recognised between tourmalines from the ŽFm and Eggenburgian beds.

Interpretation of provenance data

A high portion of metamorphic (phyllites, mica schists) clasts points to a primary source of low- to medium- grade metapelites. Phyllites reveal a low resistance to weathering and transport, which together with their blade shape and clast angularity point to a short transport and a local source. This primary source of the ŽFm was located in the adjacent Moravian Unit (Šafov and/or Lukov Group) towards the W–NW. Sandstones were redeposited from older Permo–Carboniferous deposits. The very variable heavy mineral

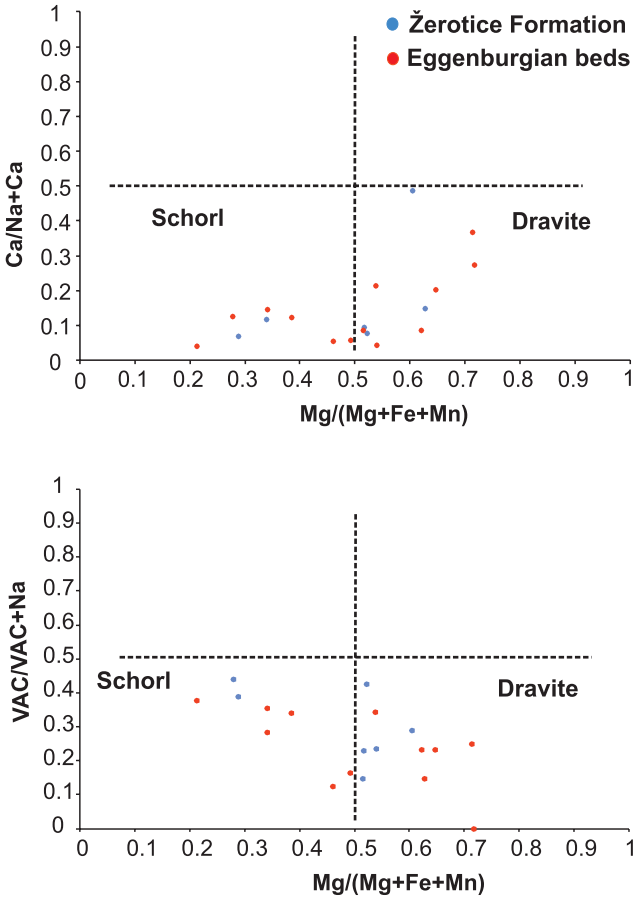

Fig. 7. Classification diagrams for studied tourmaline.

assemblages and low content of stable and low-stable heavy minerals (pyroxene, amphibole, etc.) point to relatively deeply weathered source rocks, the dominant role of the local sources and an areally restricted depositional environment. The high content of rutile and zircon (compared to tourmaline) supports redeposition from older strata. A very similar distribution of garnet types was recognised in the Permo–Carboniferous rocks of the Boskovice Basin (Nehyba et al. 2012) also with the occurrence of "exotic" andradite-grossular garnets. A source from these deposits is therefore highly probable for the ŽFm. Moreover, the Permo–Carboniferous deposits were recognised as a direct underlying rock of the ŽFm in borehole ZN-5. Short transport and redeposition from weathered bedrock is confirmed by an important content of mostly angular quartz clasts. Batík et al. (1983) described clasts of amphibolites, granites, granodiorites, and aplites in deposits of the ŽFm. The source of these rocks can also be located W to NW in the Moldanubian Unit, in the Thaya Batholith or Moravian Unit. These sources were confirmed by the study of tourmaline. The presence of garnet confirms metamorphic complexes (crystalline schists) in the source area. Zircon, tourmaline, and rutile are common in acidic to intermediate magmatic rocks, similarly to selected metamorphic rocks (von Eynatten & Gaupp 1999) and a high content of these ultrastable minerals

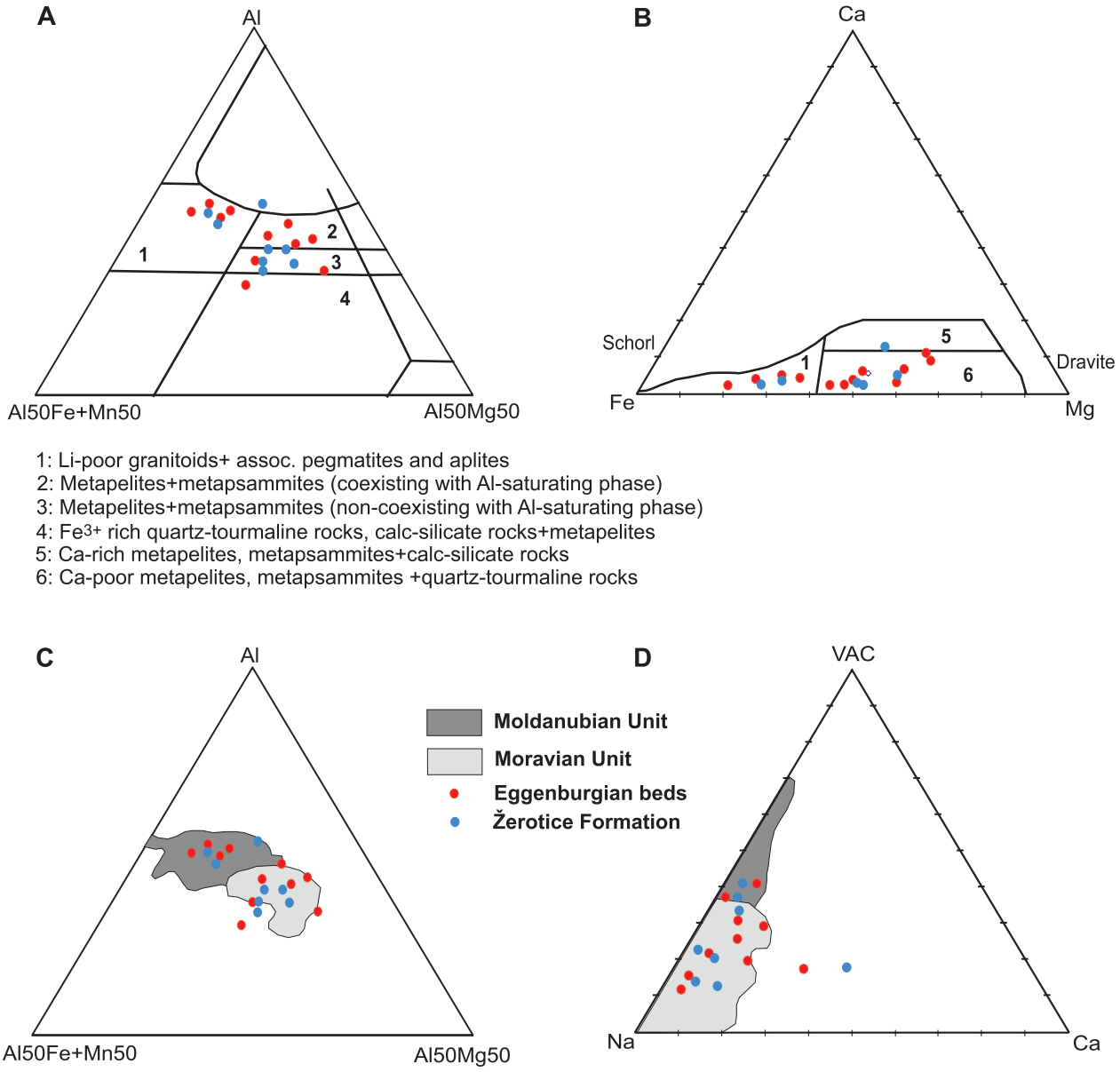

Fig. 8. Ternary discrimination diagrams for tourmaline. **A** — The Al–Fe+Mn–Mg diagram (after Henry & Guidotti 1985); **B** — the Fe–Mg–Ca diagram (after Henry & Guidotti 1985); **C** — Provenance-discrimination plot Al–Fe+Mn–Mg; **D** — provenance-discrimination plot and VAC–Na–Ca. Data from possible source rocks after Buriánek et al. (2012).

is connected with redeposition from older deposits. The zircon spectra (subordinate euhedral crystals and grains with high elongation, numerous broken crystals, etc.) rather supports the influence of a secondary/recycled source than the primary source. Generally similar zircon characteristics are known from the Permo–Carboniferous deposits of the Boskovice Basin (Nehyba et al. 2012). Recognised euhedral zircons cannot be correlated in a straightforward manner with zircons from granitoids of the Brno Massif (Leichmann & Höck 2008) or Thaya Batholith (F. Finger, personal information).

The overlying Eggenburgian beds reveal different source of pebbles and granules. The dominance of clastic sandstones and siltstones points to redeposition from older sedimentary basin infill (Mesozoic–Paleogene in age?, erosion of deposits of the ŽFm?). Simple clast spectra and a lower content of angular clasts (in favour of rounded, subrounded and subangular clasts) confirm longer transport and/or the more significant role of secondary source/redeposition. Increased content of blades and discs (at the expense of rods and spheres — if compared to the ŽFm) could reveal influence of wave action (Postma & Nemec 1990). The source area was also located W to NW in the Moldanubian and Moravian Units. These sources were also confirmed by the tourmaline study. Stable heavy mineral assemblage, higher content of stable (staurolite, garnet, apatite, etc.) minerals at the expense of ultrastable ones reveal a more uniform transportation agent/depositional environment and a significant provenance shift towards less weathered crystalline schists. The garnet–staurolite

assemblage is generally typical of lower Miocene beds of the Carpathian Foredeep and a source of staurolite is commonly traced to Cretaceous deposits according to results of Krystek (1981). Rutile studies reveal the higher influence of metamorphic rocks mostly originated from metapelites at the expense of magmatic rocks and metamafics in Eggenburgian beds compared to the ŽFm. Heavy mineral assemblages of Eggenburgian (and often also Ottnangian) beds reflect mainly metasedimentary rocks as the primary source. Nevertheless, there was a great deal of such minerals such as staurolite, kyanite, andalusite, sillimanite and partly also ultrastable rutile and tourmaline derived from residual products of weathering. The genesis of mainly kaoline deposits started in the area under study in Early Mesozoic and/or Paleogene times and was controlled by tropical wet and hot climate (Neužil et al. 1980). There are still preserved large deposits of kaolin in the close vicinity of Žerotice and Znojmo.

The dominance of almandine garnets taken on a simple level shows the provenance from gneisses and mica schists. Absolute dominance of almandine garnet is typical of the sedimentary infill of the Carpathian Foredeep (Francírek & Nehyba 2016) or of Mesozoic deposits along the eastern margin of the Bohemian Massif (Nehyba & Opletal 2016, 2017). Garnet spectra of Eggenburgian deposits is more uniform and partly different from the garnet spectra of the ŽFm. These differences can be explained by the different role of certain primary source rocks in the source area of successive beds below and above transgressive surface and a significant portion of redeposition from the Permo–Carboniferous beds for the ŽFm (see Fig. 9).

Gamma-ray spectral analysis

GRS is used for identification of lithology, grain size, sorting, processes in the source area and its composition, identification of clay minerals, content of organic matter, basin-wide correlations, identification of the depositional environment, etc. (Ruffell & Worden 2000; Akinlotan 2017).

The results of gamma-ray spectral analysis are presented in Table 4. Deposits of the ŽFm reveal relative varied gamma ray spectra. Concentrations of K are moderate to high and the high concentrations significantly predominate. Concentrations of U and the value of the Th/K vary between low to high. Concentrations of Th and the values of the Th/U ratio are all relatively high. Evaluations of concentrations are according to Hasselbo (1996). The Th and K concentrations show a relatively high positive correlation (linear regression coefficient; R=0.67), similarly to concentrations of K and U (R=0.64). Correlation between the concentrations of Th and U is slightly lower (R=0.42). The SGR value shows a very high correlation to values of U (R=0.92), K (R=0.83) and also Th (R=0.79). Low to high negative correlations between K (R=−0.25),

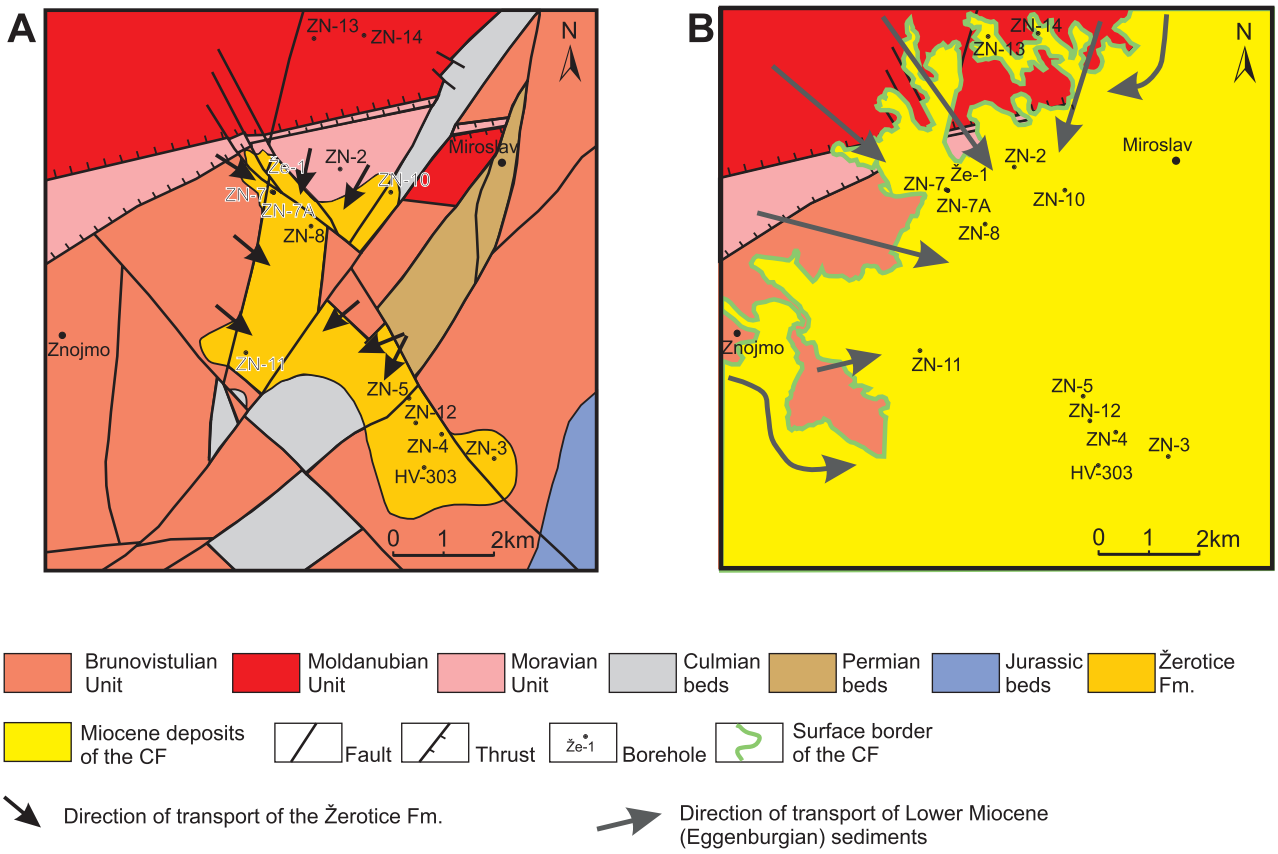

Fig. 9. Interpreted source area for the studied beds of the Žerotice Formation (**A**) and for the overlying Eggenburgian beds (**B**).

Table 4: Results of gamma-ray spectral analysis.

Facies associations	K [%]		U (ppm)		Th (ppm)		SGR [API]		Th/K		Th/U	
	AVG (Min–Max)	SD	AVG (Min-Max)	SD	AVG (Min-Max)	SD	AVG (Min-Max)	SD	AVG (Min-Max)	SD	AVG (Min-Max)	SD
FA 1+2	3.1 (1.8–4.3)	0.8	4.3 (2.5–7.8)	1.7	14.3 (10.3–20.7)	2.8	142.0 (94.0–199.7)	31.1	4.8 (3.1–7.1)	1.1	3.6 (2.2–6.3)	1.1
FA 3	2.0 (1.4–3.0)	0.5	3.5 (1.5–6.4)	1.5	7.8 (3.4–10.8)	2.7	92.0 (56.0–126.7)	25.0	4.4 (1.1–6.3)	1.6	3.2 (1.1–6.3)	1.6

Th (R=−0.82), U (R=−0.29) and clay content, similar negative correlations between K (R=−0.71), Th (R=−0.85), U (R=−0.53) and silt fraction vs. high positive correlations between K (R=0.64), Th (R=0.87), U (R=0.50) and sand fraction clearly reflect that the dominant hosting minerals of these radio elements are contained in the sand fraction.

Concentrations of K and Th of the overlying Eggenburgian deposits are moderate and high. Concentrations of U can be evaluated as low to high. The values of both the Th/K and Th/U ratios vary significantly from low to high values. Evaluations of concentrations are according to Hasselbo (1996). Correlation between the concentrations of K and U are relatively low (R=0.38), similarly like correlation between U and Th (R=0.31). On the other hand, correlation between K and Th is high (R=0.73). The value of total radioactivity SGR shows very high correlation to values of K (R=0.83), Th (R=0.82) and also U (R=0.75).

Interpretation: Recognized concentrations of radioactive elements are mostly higher than known data from deposits of the Carpathian Foredeep (Holcová et al. 2015; Nehyba et al. 2016; Kopecká et al. 2018). Significant correlations between "total radioactivity" SGR and concentrations of K, Th and U together with correlations between individual elements (especially Th vs. K) point to common source or signal. It is obvious that the total radioactivity and the concentrations of all radiometric elements are significantly higher and in wider ranges in the ŽFm than in the overlying Eggenburgian deposits. Especially the higher K and Th contents are related to a greater volume of clay minerals in the deposits of the ŽFm. Overlaying Eggenburgian deposits are mostly sands. The very high concentration of Th in the ŽFm points to a significant role of kaolinite in the studied samples. The relatively high content of U in some samples from the ŽFm can be explained by the material provenance (redeposited Cretaceous or Permian deposits?). High variation in the gamma ray values in the deposits of the ŽFm points to high variations in their lithology and possibly also to variations in the source and weathering processes.

According to Doveton & Merriam (2004), the Th/K ratio can be applied to the recognition of clay minerals and distinction of micas and K-feldspars. Similar values of Th/K ratio and its high variability implied high variations in both unstable and stable minerals in the samples studied. This result reveals high differences in the mineral maturity of the studied samples.

The U versus Th plot (Fig. 10A) indicates that whereas most of the Eggenburgian samples experienced authigenic enrichment in U, the majority of the ŽFm samples is located below the separation line. The authigenic enrichment of U is explained mostly by a higher content of organic matter, whereas the points below the lines correspond to samples, which have no significant organic matter (Myers & Wignall 1987).

The Th/U ratio has also proved to be useful in the recognition of geochemical facies or as an indicator of the redox-potential (Myers & Wignall 1987; Doveton 1991) or even the depositional environment (Adams & Weaver 1958). The cross plot of Th/K versus Th/U ratios is presented in Fig. 10B. Higher values of especially the Th/U ratio and also Th/K for samples from the ŽFm are obvious. It is explained by an evidence of a more oxidic condition during their deposition then in the overlying Eggenburgian beds. This result supports terrestrial depositional environments for the ŽFm, because the Eggenburgian deposits are clearly shallow marine and nearshore deposits. Deposits reveal a character of mixed clay structures, with a higher role of kaolinite for samples from the ŽFm. Some

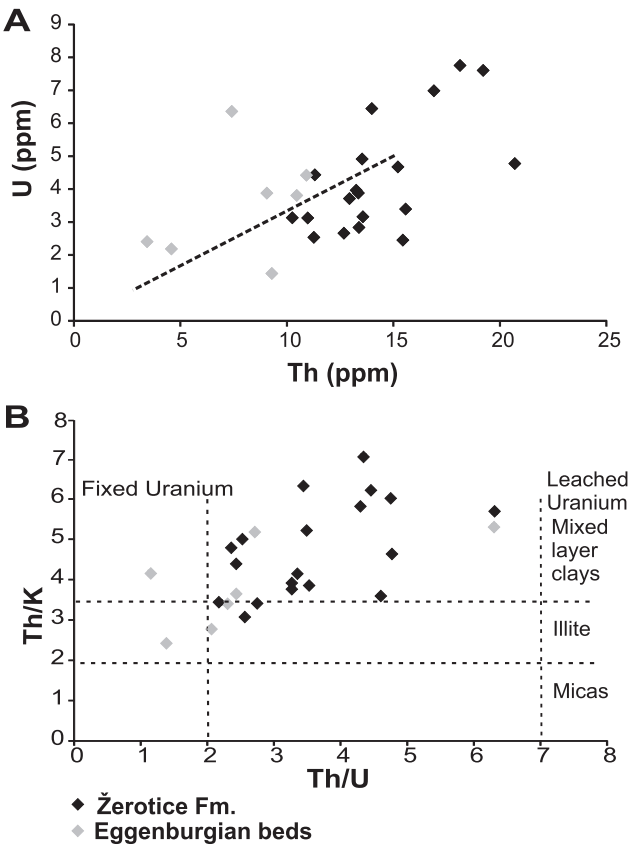

Fig. 10. Results of gamma-ray spectral analysis. **A** — Crossplot of U versus Th with discrimination line Th/U=2; **B** — crossplot of Th/K versus Th/U ratios showing the redox-condition of studied deposits.

variations can be explained by different weathering processes in the source area (Ruffell & Worden 2000; Schnyder et al. 2006). The higher content of kaolinite can be connected with a source from highly weathered and kaolinized crystalline rocks.

Discussion

The sedimentary infill of the Žerotice paleovalley generally resembles models of estuarine incised-valley systems with three-fold vertical and longitudinal diversification (Dalrymple et al. 1994). These are — the basal/inner valley segment comprising alluvial/fluvial deposits (i.e. FA1), diversified facies distribution in the middle segment (i.e. FA 2) and the outer/upper segment under the strong influence of nearshore marine processes (i.e. FA 3). The actual distribution of depositional environments is dependent on the rates of sediment supply and formation of accommodation space. The significant role of "muddy central infill" of the valley i.e. FA 2 in the ŽFm lithology points to a gradual base-level rise combined with a relatively low coarse-sediment supply, results i.e. the classic 'underfilled' estuary (Zaitlin et al. 1994; Gobo et al. 2014). The proposed model of deposition of the ŽFm is presented in Fig. 11.

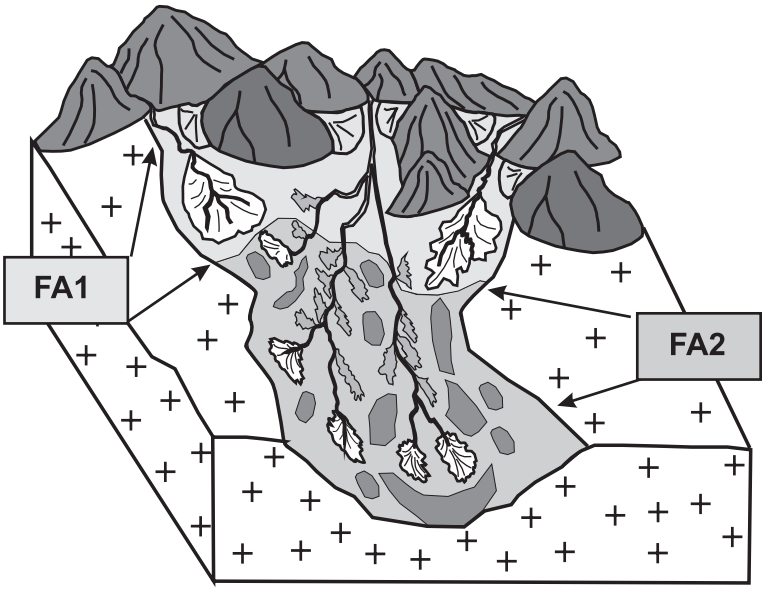

Fig. 11. Schematic model of the possible depositional environment of the Žerotice Formation and position of facies association FA 1 and FA 2.

The preservation of floodbasin strata is typically related to the establishment of negative floodplain topography protected from channel erosion (Lewin & Ashworth 2014). This could have been the result of basin subsidence (Jorgensen & Fielding 1996). However, most rock units hosting a volumetrically significant proportion of floodplain deposits accumulated in tectonic realms (Ielpi et al. 2018). The local confined preservation of the ŽFm is therefore preliminarily explained as deposition in a tectonically confined paleovalley. The formation of accommodation space for the ŽFm in this paleovalley is interpreted as a result of bedrock fault reactivation (Waschbusch & Royden 1992). Evidence for such a tectonically predisposed valley seems to be supported by the preservation of Permo–Carboniferous clastics and Devonian carbonates within the paleovalley (surrounded by crystalline rocks) and common intense brittle deformation of Miocene beds (facies T). Reactivation of the faults and formation of accommodation space for the ŽFm might be connected with orogenic processes in the Eastern Alps during the Eocene–Oligocene (Kuhlemann & Kempf 2002; Schuster & Stüwe 2010). The eustatic or relative sea-level fluctuations could further modify the valley extend and infill.

Classic models for peripheral foreland basin formation and development (Beaumont 1981; Flemings & Jordan 1989; Crampton & Allen 1995; DeCelles & Giles 1996; Sinclair 1997; Leszczyński & Nemec 2015, etc.) connect processes along the passive/distal cratonward basin margin with flexural bending of the lithosphere due to tectonic loading and with formation and evolution of the peripheral forebulge. Evidence of the relatively thick terrestrial and estuarine ŽFm deposits below the marine Eggenburgian sediments confirms that the formation of the depositional space directly preceded the Eggenburgian marine transgression. The proven local source of deposits of the ŽFm, evidence of basal alluvial wedge/FA1 and deposition in a narrow confined area, point to the erosion of structurally controlled topography (Postma 1984; Breda et al. 2007; Ford et al. 2007; Rohais et al. 2008). Accommodation in alluvial systems is typically controlled by a tectonic uplift of the source area, paleotopography, the geology of the drainage basin and climate (Shanley & McCabe 1994; Gupta 1999; Viseras et al. 2003; Andreucci et al. 2014). Such deposition is therefore commonly unrelated to the sea-level variations and therefore it is difficult to characterize deposits of the ŽFm in the terms of sequence stratigraphic terminology, which is also complicated by their enigmatic stratigraphy. The top part of the deposits of the ŽFm (FA 2) might be assigned as "Early transgressive systems tracts" (Koss et al. 1994; Shanley & McCabe 1994; Nehyba 2000), especially due to areally restricted preservation, prevalent vertical accretion, lagoonal to distal flood plain deposition and direct position below "the main" transgressive surface. Such an interpretation might be supported by a back-stepping stratigraphic succession represented by a successive train of FA1, FA 2 and Eggenburgian beds/FA 3. It is widely accepted that the initial subsidence of the western margin of the southern segment of the MCF occurred in the Egerian (Brzobohatý & Cicha 1993; Nehyba & Šikula 2007). Therefore, these deposits might be probably Egerian in age. The base of overlying Eggenburgian beds represents a sequence boundary i.e. flexurally induced transgressive surface/basal forebulge unconformity. Eggenburgian beds are onlaping on deposits of the ŽFm.

The proven provenance from Permo–Carboniferous deposits (for the deposits of the ŽFm) and the higher content of staurolite in heavy mineral spectra of the overlaying marine Eggenburgian beds (redeposited from Cretaceous beds?) reveals that both Paleozoic and Mesozoic sedimentary rocks had a significantly higher areal extent in the area under study than is currently known, and that the basal forebulge unconformity represents a significant change in provenance, paleodrainage and paleotopography.

Conclusions

The Žerotice Formation, as a basal unit of the sedimentary succession of the southwestern margin of the Carpathian Foredeep (Moravia, Czech Republic), was recognised in the confined area NE–SE of Znojmo. Revision of the borehole data shows that thickness of the Žerotice Formation highly varies (up to more than 60 m). Two facies associations were recognised within the Žerotice Formation. The first facies association mantles the pre-Neogene basement with an irregular unconformity and is interpreted as alluvial to fluvial deposits. These deposits are a product of generally arid climatic conditions and flashy discharge of episodic shallow, high-energy stream flows and/or mass flows. They reveal enigmatic stratigraphy and their deposition was controlled by tectonics, paleotopography and climate. They might be unrelated to the sea-level variations, so it is difficult to characterize them in terms of sequence stratigraphic terminology. The second facies association is interpreted as lagoonal to distal flood plain deposits. The unfossiliferous deposits of the Žerotice Formation are covered by the nearshore marine Eggenburgian deposits. The boundary between these beds represents a sequence boundary (i.e. the basal forebulge unconformity).

Detailed provenance studies of successive beds below and above this sequence boundary showed differences in the source area and paleodrainage. Both the local primary crystalline rocks and older sedimentary cover form the source area of the Žerotice Formation. The crystalline rocks were represented mostly by low- to medium-grade metapelites of the adjacent Moravian Unit. Further sources were formed by the metamorphics of the Moldanubian Unit and granitoids of the Thaya Batholith. All these geological units are located only a few km in a NW direction, very close to the preserved deposits of the Žerotice Formation. Very significant for provenance were Permo–Carboniferous sedimentary rocks. Short transport and a local source from intensely weathered bedrock was proved. Deposits of the Žerotice Formation reveal increased concentrations of natural radioactive elements if compared to the sedimentary infill of the Carpathian Foredeep. The source area of the overlying marine Eggenburgian beds was located W to NW in the Moldanubian and Moravian Units. More stable heavy mineral assemblage and the greater role of stable (staurolite, garnet) minerals at the expense of ultrastable ones reveal a more uniform depositional environment, a provenance shift towards less weathered crystalline schists, longer transport and wave action. The metamorphic rocks (especially metapelites) highly prevail in the source area at the expense of magmatic rocks and Paleozoic deposits if compared to the Žerotice Formation. A possible source from the older Cretaceous deposits is supposed for the Eggenburgian beds due to significant content of staurolite. A significantly broader (and more distant) source area is therefore interpreted for these marine deposits if compared to the deposits of the Žerotice Formation. Local confined preservation of the Žerotice Formation is preliminarily explained as being connected with a tectonically predisposed paleovalley.

Acknowledgements: This work was supported by the Ministry of Regional Development of the Czech Republic (project INTERREG V-A Austria–Czech Republic — Hydrothermal potential of the area — ATCZ167). We are obliged to thanks Petr Gadas for help with management of tourmaline data. Support was also provided by the project No. 321070 of the Czech Geological Survey, project leader Oldřich Krejčí. The manuscript benefited from the reviews of Reinhard Roetzel, Samuel Rybár and two unknown reviewers. Mr. Christopher A. Rance, M.A. is thanked for the English correction.

References

Adámek J. 2003: The Miocene of the Carpathian Foredeep in southern Moravia, geological development and lithostratigraphic classification. *Zprávy o geologických výzkumech v r. 2002,* 9–11 (in Czech).

Adámek J., Brzobohatý R., Pálenský P. & Šikula J. 2003: The Karpatian in the Carpathian Foredeep (Moravia). In: Brzobohatý R., Cicha I., Kováč M. & Rögl F. (Eds.): The Karpatian, a Lower Miocene Stage of the Central Paratethys. *Masaryk University*, Brno, 75–92.

Adams J.A.S. & Weaver E. 1958: Thorium to uranium ratios as indicators of sedimentary process: example of concept of geochemical facies. *AAPG Bulletin* 42, 387–430.

Akinlotan O. 2017: Geochemical analysis for paleoenvironmental interpretations — a case study of the English Wealden (Lower Cretaceous, south-east England). *Geol. Quarterly* 61, 1, 227–238.

Andreucci S., Panzeri L., Martini P., Maspero F., Martini M. & Pascucci V. 2014: Evolution and architecture of a West Mediterranean Upper Pleistocene to Holocene coastal Apron-fan system. *Sedimentology* 61, 2, 333–361.

Aubrecht R., Méres Š., Sýkora M. & Mikuš T. 2009: Provenance of the detrital garnets and spinels from the Albian sediments of the Czorsztyn Unit (Pieniny Klippen Belt, Western Carpathians, Slovakia). *Geol. Carpath.* 60, 463–483.

Baker V.R. 1984: Flood sedimentation in bedrock fluvial systems. In: Koster E.H. & Steel R.J. (Eds.): Sedimentology of Gravels and Conglomerates. *Canadian Society of Petroleum Geologists*, *Memoir* 10, 87–98.

Batík P., Čtyroký P., Gabriel M., Holásek O., Klečák J., Líbalová J., Mátl V., Matějovská O., Střída M., Šalanský K., Štych J. & Zeman A. 1983: Explanations to the geological map of ČSSR 1:25,000. Znojmo, 34-113. *Ústřední ústav geologický*, Praha (in Czech).

Beaumont C. 1981: Foreland basins. *Geoph. Journal of the Royal Astronomical Society* 55, 291–329.

Blair T.C. 1999: Cause of the dominance by sheetflood vs. debris-flow processes on two adjacent alluvial fans, Death Valley, California. *Sedimentology* 46, 1015–1025.

Breda A., Mellere D. & Massari F. 2007: Facies and processes in a Gilbert-delta-filled incised valley (Pliocene of Ventimiglia, NW Italy). *Sediment. Geol.* 200, 31–55.

Bridge J.S. & Demicco R. 2008: Earth Surface Processes, Landforms and Sediment Deposits. *Cambridge University Press*, Cambridge, 1–815.

Brzobohatý R. 2002: The Carpathian Foredeep. In: Geological history of the Czech Republic. *Academia*, Praha, 346–353 (in Czech).

Brzobohatý R. & Cicha I. 1993: The Carpathian Foredeep. In: Přichystal A., Obstová V. & Suk M. (Eds.): Geologie Moravy a Slezska. *MZM a PřF MU,* Brno, 123–128 (in Czech).

Buriánek D., Tomanová Petrová P. & Otava J. 2012: Where do the Miocene sediments of the Brno region come from? *Acta Musei Moraviae, Sci. Geology* 97, 1, 153–156 (in Czech).

Collinson J., Mountney N. & Thompson D. 2006: Sedimentary Structures. *Terra Publishing*, Harpenden, Hertfordshire, England. 1–292.

Crampton S.L. & Allen P.A. 1995: Recognition of forebulge unconformities associated with early stage foreland basin development: example from the north Alpine foreland basin. *AAPG Bull*. 79, 1495–1514.

Čopjaková R., Sulovský P. & Otava J. 2002: Comparison of the chemistry of detritic pyrope-almandine garnets of the Luleč Conglomerates with the chemistry of granulite garnets from the Czech Massif. *Geologické výzkumy na Moravě a ve Slezku v roce 2001*, 9, 44–47 (in Czech).

Čtyroký P. 1982: Lower Miocene (Eggenburgian and Ottnangian) of sw. part of the Carpathian Foredeep in Moravia. *Zem. Plyn Nafta* 27, 4, 379–394 (in Czech).

Čtyroký, P. 1991: Classification and correlation of the Eggenburgian and Ottnangian in the south part of the Carpathian Foredeep in South Moravia. *Záp. Karpaty. sér. geol.* 15, 67–109 (in Czech).

Čtyroký P. 1993: The Tertiary on Bohemian Massif in South Moravia. *Jahrb. Geol. Bundesanst.* 136, 4, 707–713.

Dalrymple R.W. 2004: Incised valleys in time and space: an inroduction to the volume and examination of the controls on valley formation and filling. In: Dalrymple R.W., Lecke D.A. & Tillman R.W. (Eds.): Incised valleys in time and space. *SEPM Spec. Publ.* 85, 5–12.

Dalrymple R.W., Boyd R. & Zaitlin B.A. (Eds.) 1994: Incised-valley systems: origin and sedimentary sequences. *SEPM Spec. Publ.* 51, 391.

DeCelles P.G. & Giles K.A. 1996: Foreland basin systems. *Basin Research* 8, 105–123.

Dietrich P., Ghienne F., Schuster M., Lajeunesse P., Nutz A., Deschamps R., Roquin C. & Duringer P. 2017: From outwash to coastal systems in the Portneuf–Forestvilledeltaic complex (Quebec North Shore): Anatomy of a forcedregressive deglacial sequence. *Sedimentology* 64, 1044–1078.

Dlabač M. 1976: Neogene on the se. margin of the Bohemian–Moravian Highlands. *Výzk. Práce. Ústř. Úst. geol*. 13, 7–21 (in Czech).

Doveton J.H. 1991: Lithofacies and geochemical facies profiles from nuclear wireline logs: new subsurface templates for sedimentary modelling. In: Franseen E.K., Watney W.L., Kendall C.J. & Ross W. (Eds.): Sedimentary modelling-computer simulations and methods for improved parameter definition. *Kansas Geological Society Bulletin* 233, 101–110.

Doveton J.H. & Merriam D.F. 2004: Borehole petrophysical chemostratigraphy of Pennsylvanian black shales in the Kansas subsurface. *Chem. Geol.* 206, 249–258.

Fernández L.P., Agueda J.A., Colmenero J.R., Salvador C.I. & Barba P. 1988: A coal-bearing fan-delta complex in the Westphalian D of the Central Coal Basin, Cantabrian Mountains, northwestern Spain: imlications for the recognition of humid-type fan deltas. In: Nemec W. & Steel R.J. (Eds.): Fan Deltas: Sedimentology and Tectonic Settings. *Blackie and Son*, 286–302.

Fielding C.R. 1985: Coal depositional models and the distinction between alluvial and delta plain environments. *Sediment. Geol.* 42, 41–48.

Finger F. & Haunschmid B. 1988: Die mikroskopische Untersuchung der akzessorischen Zirkone als Methode zur Klärung der Intrusionsfolge in Granitgebieten — eine Studie im nordöstlichen oberösterreichischen Moldanubikum. *Jahrb. Geol. Bundesanst.* 131, 2, 255–266.

Flemings P.B. & Jordan T.E. 1989: A synthetic stratigraphic model of foreland basin development. *J. Geophys. Res.* 94, B4, 3851–3866.

Folk R.L. & Ward W. 1957: Brazos River bar: a study in the significance of grain-size parameters. *J. Sediment. Petrol.* 27, 3–26.

Force E.R. 1980: The provenance of rutile. *J. Sediment. Res.* 50, 2, 485–488.

Ford M., Williams E.A., Malartre F. & Popescu S.M. 2007: Stratigraphic architecture, sedimentology and structure of the Vouraikos Gilbert-type fan delta, Gulf of Corinth, Greece. In: Nichols G., Williams E. & Paola C. (Eds.): Sedimentary Processes, Environments and Basins. A Tribute to Peter Friend. *Int. Assoc. Sedimentol. Spec. Publ.* 38, 49–90.

Fralick P. & Zaniewski K. 2012: Sedimentology of a wet, pre-vegetation floodplain assemblage. *Sedimentology* 59, 1030–1049.

Francírek M. & Nehyba S. 2016: Evolution of the passive margin of the peripheral foreland basin: an example from the Lower Miocene Carpathian Foredeep (Czech Republic). *Geol. Carpath*. 67, 1, 39–66.

Gobo K., Ghinassi M., Nemec W. & Sjursen E. 2014: Development of an incised valley-fill at an evolving rift margin: Pleistocene eustasy and tectonics on the southern side of the Gulf of Corinth, Grece. *Sedimentology* 61, 1086–1119.

Głuszy'nski A. & Aleksandrowski P. 2016: A deep palaeovalley in the floor of the Polish Carpathian Foredeep Basin near Pilzno and its control on Badenian (Middle Miocene) evaporite facies. *Geol. Quarterly* 60, 2, 493–516.

Gupta S. 1999: Controls on sedimentation in distal margin palaeovalleys in the Early Tertiary Alpine foreland basin, south-eastern France. *Sedimentology* 46, 357–384.

Hampton B.A. & Horton B.K. 2007: Sheetflow fluvial processes in a rapidly subsiding basin, Altiplano plateau, Bolivia. *Sedimentology* 54, 1121–1148.

Henry D.J. & Guidotti C.V. 1985: Tourmaline as a petrogenetic indicator mineral: An example from the staurolite-grade metapelites of NW Maine. *Am. Mineral.* 70, 1–15.

Hasselbo S.P. 1996: Stratigraphy, Cenozoic of the Atlantic margin, offshore New Jersey. In: Mountain G.S., Miller K.G., Blum P., Poag C.W. & Twichell D.C. (Eds.): Proceedings of the Ocean Drilling Program. *Scientific Results* 150, 411–422.

Holcová K., Hrabovský J., Nehyba S., Hladilová Š., Doláková N. & Demény A. 2015: The Langhian (Middle Badenian) carbonate production event in the Moravian part of the Carpathian Foredeep (Central Paratethys): a multiproxy record. *Facies* 61, 1.

Hoppe G. 1966: Zirkone aus Granuliten. *Berichte der Deutschen Gesellschaft für Geologische Wissenschaften – Reihe B: Mineralogie und Lagerstättenforschung* 11, 1, 47–81.

Hubert J.F. 1962: A zircon-tourmaline-rutile maturity index and the interdependence of the composition of heavy mineral assemblages with the gross composition and texture of sandstones. *J. Sediment. Res*. 32, 3, 440–450.

Ielpi A., Fralick P., Ventrac D., Ghinassi M., Lebeaua L-E., Marconato A., Meeka R. & Rainbirdfet R.H. 2018: Fluvial floodplains prior to greening of the continents: Stratigraphic record, geodynamic setting, and modern analogues. *Sediment. Geol.* 372, 140–172.

Jarosiñski, M., Poprawa, P. & Ziegler, P.A. 2009: Cenozoic dynamic evolution of the Polish Platform. *Geol. Quarterly* 53, 1, 3–26.

Jorgensen P.J. & Fielding C.R. 1996: Facies architecture of alluvial floodbasin deposits: three-dimensional data from the Upper Triassic Callide coal measures of eastcentral Queensland, Australia. *Sedimentology* 43, 479–495.

Jucha S. 1985: New features of structure of the Carpathian Foredeep and basement of the Carpathians. *Przegląd Geologiczny* 33, 333–344 (in Polish with English summary).

Karnkowski P. 1989: Deltaic deposits of the Carpathian foreland. *Przegląd Geologiczny* 37, 28–32 (in Polish with English summary).

Karnkowski P.H. & Ozimkowski W. 2001: Structural evolution of the pre-Miocene basement in the Carpathian Foredeep (Kraków–Przemyśl region, SE Poland). *Przegląd Geologiczny* 49, 431–436 (in Polish with English summary).

Kempf O. & Pfiffner O.A. 2004: Early Tertiary evolution of the North Alpine Foreland Basin of the Swiss Alps and adjoining areas. *Basin Res.* 16, 549–567.

Kopecká J., Holcová K., Nehyba S., Hladilová Š., Brzobohatý R. & Bitner M.A. 2018: The earliest Badenian Planostegina bloom deposit: reflection of an unusual environment in the westernmost Carpathian Foredeep (Czech Republic). *Geol. Quarterly* 62, 1, 18–37.

Koss J.E., Ethridge F.G. & Schumm S.A. 1994: An experimental study of the effect of base-level change on fluvial, coastal and shelf systems. *J. Sediment. Res.* B64, 90–98.

Krejčí O., Ambrozek V., Bubík M., Drábková J., Gilíková H., Kryštofová E., Otava J., Tomanová Petrová P., Švábenická L., Hubatka F., Nehyba S. & Kuda F. 2017: Definition of the Žerotice trough in the Znojmo Region and valuing its perspectives from groundwater resources point of view. Final report. *Open File Report, MS Archives CGS*, Prague, 1–49 (in Czech).

Krystek I. 1981: Using of assemblages of heavy minerals in sedimentary complexes. *Folia Univ. Purkyn. Brunn*., *Geologia* 22, 3, 101–107 (in Czech).

Krystková L. & Krystek I. 1981: New data from hydrogeology dril holes in SW part of the Carpathian Foredeep in Moravia. *Scripta Univ. Purkyn. Brunn., Geologia* 11, 2, 73–80.

Krzywiec P. 1997: Large-scale tectono-sedimentary Middle Miocene history of the central and eastern Polish Carpathian Foredeep Basin — results of seismic data interpretation. *Przegląd Geologiczny* 45, 1039–1053.

Krzywiec P. 2001: Contrasting tectonic and sedimentary history of the central and eastern parts of the Polish Carpathian Foredeep basin – results of seismic data interpretation. *Mar. Petrol. Geol.* 18, 13–38.

Kuhlemann J. & Kempf O. 2002: Post-Eocene evolution of the North Alpine Foreland Basin and its response to Alpine tectonics. *Sediment. Geol.* 152, 45–78.

Leichmann J. & Höck V. 2008: The Brno Batholit: an insight into the magmatic and metamorphic evolution of the Cadomian Brunovistulian Unit, eastern margin of the Bohemian Massif. *J. Geosci.* 53, 281–305.

Leszczyński S. & Nemec W. 2015: Dynamic stratigraphy of composite peripheral unconformity in a foredeep basin. *Sedimentology* 62, 645–680.

Lewin J. & Ashworth P.J. 2014: The negative relief of large river floodplains. *Earth-Sci. Rev.* 129, 1–23.

Lihou J.C. & Mange-Rajetzky M.A. 1996: Provenance of the Sardona Flysch, eastern Swiss Alps: example of high-resolution heavy mineral analysis applied to an ultrastable assemblage. *Sediment. Geol*. 105, 141–157.

Lottes A.L. & Ziegler A.M., 1994: World peat occurrence and the seasonality of climate and vegetation. *Palaeogeogr. Palaeoclimatol. Palaeoecol.* 106, 23–37.

Lowe D.R. 1982: Sediment gravity flows: II. Depositional models with special reference to the deposits of high-density turbidity currents. *J. Sediment. Petrol.* 52, 279–297.

Mader D. 1980: Weitergewachsene Zirkone im Bundsandstein der Westeifel. *Der Aufschluss* 31, 163–170.

Mange M.A. & Morton A.C. 2007: Geochemistry of heavy minerals. In: Mange M.A. & Wright D.T. (Eds.): Heavy Minerals in Use. *Developments in Sedimentology* 58, 345–391.

Marconato A., Almeida R.P., Turra B.B. & Fragoso-Cesar A.R.S. 2014: Pre-vegetation fluvial floodplains and channel-belts in the Late Neoproterozoic-Cambrian Santa Bárbara Group (Southern Brazil). *Sediment. Geol.* 300, 49–61.

Meinhold G., Anders B., Kostopoulos D. & Reischmann T. 2008: Rutile chemistry and thermometry as provenance indicator: An example from Chios Island, Greece. *Sediment. Geol.* 203, 98–111.

Méres S. 2008: Garnets — important information resource about source area and parental rocks of the siliciclastic sedimentary rocks. In: Jurkovič L. (Ed.): Cambelove dni 2008, Geochémia — Základná a aplikovaná geoveda. *UK,* Bratislava, 37–43 (in Slovak).

Mertz K.A. & Hubert J.F. 1990: Cycles of sand-flat sandstone and playa-lacustrine mudstone in the Triassic-Jurassic Blomidon redbeds, Fundy rift basin, Nova Scotia: implications for tectonic and climatic implications. *Can. J. Earth Sci.* 27, 442–451.

Morton A.C. 1984: Stability of detrital heavy minerals in Tertiary sandstones from the North Sea Basin. *Clay Miner*. 19, 287–308.

Morton A.C. & Hallsworth C. 1994: Identifying provenance-specific features of detrital heavy mineral assemblages in sandstones. *Sediment. Geol.* 90, 241–256.

Mulder T. & Alexander J. 2001: The physical character of subaqueous sedimentary density flows and their deposits. *Sedimentology* 48, 269–299.

Myers K.J. & Wignall P.B. 1987: Understanding Jurassic organic-rich mudrocks-new concepts using gamma-ray spectrometry and palaeoecology: examples from the Kimmeridge Clay of Dorset and the Jet Rock of Yorkshire. In: Legget J.K. & Zuffa G.G. (Eds.): Marine clastic sedimentology. *Graham and Trotman*, London, 172–189.

Nehyba S. 2000: The cyclicity of Lower Miocene deposits of the SW part of the Carpathian Foredeep as the depositional response to sediment supply and sea-level changes. *Geol. Carpath.* 51, 1, 7–17.

Nehyba S. & Opletal V. 2016: Depositional environment and provenance of the Gresten Formation (Dogger) on the southeastern slopes of the Bohemian Massif (Czech Republic, subsurface data). *Austrian J. Earth Sci.* 109, 2.

Nehyba S. & Opletal V. 2017: Sedimentological study of the Nikolčice Formation — evidence of the Middle Jurassic transgression onto the Bohemian Massif (subsurface data). *Geol. Quarterly* 61, 1, 138–155.

Nehyba S. & Roetzel R. 2010: Fluvial deposits of the St. Marein–Freischling Formation — insights into initial depositional processes on the distal external margin of the Alpine-Carpathian Foredeep in Lower Austria. *Austrian J. Earth Sci.* 103, 2, 50–80.

Nehyba S. & Roetzel R. 2015: Depositional environment and provenance analyses of the Zöbing Formation (Upper Carboniferous–Lower Permian), Austria. *Austrian J. Earth Sci.* 108, 2, 245–276.

Nehyba S. & Šikula J. 2007: Depositional architecture, sequence stratigraphy and geodynamic development of the Carpathian Foredeep (Czech Republic). *Geol. Carpath.* 58, 1, 53–69.

Nehyba S., Roetzel R. & Adamová M. 1999: Tephrostratigraphy of the Neogene volcaniclastics (Moravia, Lower Austria, Poland). *Geol. Carpath.* 50, Spec. Iss. 126–128.

Nehyba S., Roetzel R. & Maštera L. 2012: Provenance analysis of the Permo-Carboniferous fluvial sandstones of the southern part of the Boskovice Basin and the Zöbing Area (Czech Republic, Austria): implications for paleogeographical reconstructions of the post-Variscan collapse basins. *Geol. Carpath.* 63, 365–382.

Nehyba S., Holcová K., Gedl P. & Doláková N. 2016: The Lower Badenian transgressive-regressive cycles — a case study from Oslavany (Carpathian Foredeep, Czech Republic). *Neues Jahrb. Geol. Paläontol.* 279, 2, 209–238.

Nemec W. & Steel R.J. 1984: Alluvial and coastal conglomerates: their significant features and some comments on gravelly mass-flow deposits. In: Koster E.H. & Steel R.J. (Eds.): Sedimentology of Gravels and Conglomerates. *Can. Soc. Petrol. Geol. Memoir* 10, 1–31.

Neužil J., Kužvart M. & Šeba P. 1980: Kaolinization of the rock of the Thaya Batholith. *Sbor. geol. Věd, řada LG* 21, 7–41 (in Czech)

Nichols G.J. & Fisher J.A. 2007: Processes, facies and architecture of fluvial distributary system deposits. *Sediment. Geol.* 195, 75–90.

Oszczypko N. & Ślączka A. 1985: An atempt to palinspastic reconstruction of Neogene basins of the Carpathian Foredeep. *Annales Societatis Geologorum Poloniae* 55, 55–75.

Oszczypko N. & Tomaś A. 1976: Pre-Tortonian relief of the Carpathian Foreland between Kraków and Dębica and its effect on Miocene sedimentation. *Rocznik Polskiego Towarzystwa Geologicznego*. 46, 525–548 (in Polish with English summary).

Oszczypko N., Krzywiec P., Popadyuk I. & Peryt T. 2006: Carpathian Foredeep Basin (Poland and Ukraine): its sedimentary, structural, and geodynamic evolution. *AAPG Memoir* 84, 261–318.

Otava J., Sulovský P. & Čopjaková R. 2000: Provenance changes of the Drahany Culm greywackes: statistical evaluation. *Geologické výzkumy na Moravě a ve Slezku v r. 1999*, Brno, 94–98 (in Czech).

Picha F. 1979: Ancient submarine canyons of Tethyan continental margins, Czechoslovakia. *AAPG Bulletin* 63, 67–86.

Picha F., Stráník Z. & Krejčí O. 2006: Geology and hydrocarbon resources of the Outer Western Carpathians and their foreland, Czech Republic. *AAPG Memoir* 84, 49–175.

Poldervaart A. 1950: Statistical studies of zircon as a criterion in granitization. *Nature* 165, 574–575.

Połtowicz S. 1998: Middle-Badenian submarine erosion in Carpathian Foreland. Exploratory implications. *Nafta-Gaz* 54, 209–215 (in Polish with English summary).

Postma G. 1984: Mass-flow conglomerates in a submarine canyon: abrioja fan delta, Pliocene, Southeast Spain. In: Koster E.H. & Steel R.J. (Eds.): Sedimentology of Gravels and Conglomerates, *Canadian Society of Petroleum Geologists, Memoir* 10, 237–258.

Postma G. & Nemec W. 1990: Regressive and transgressive sequences in a raised Holocene gravelly beach, southwestern Crete. *Sedimentology* 37, 907–920.

Powers M.C. 1982: Comparison chart for estimating roundness and sphericity. *AGI Data Sheet* 18.

Prachař L. 1970: Final report about the results of the drill prospection in Miocene of the Carpathian Foredeep between Miroslav, Znojmo and Hrušovany nad Jevišovkou. *Open File Report, ČGS-Geofond,* Praha (in Czech).

Pupin J.P. 1980: Zircon and Granite Petrology. *Contrib. Mineral. Petrol*. 73, 207–220.

Pupin J.P. 1985: Magmatic zoning of hercynian granitoids in France based on zircon typology. *Schweiz. Mineral. Petrograph. Mitt.* 65, 29–56.

Rider M. 1996: The Geological Interpretation of Wireline Logs. *Whittles*, Caithness, 1–175.

Roetzel R. 2002: Legende un kurtze erläuterung zur Geologische Karte von Niederösterreich 1:200,000. In: Schnabel W., Krenmayer H-G., Mandl G.W., Novotny A., Roetzel R., Scharbert S. &. Schnabel W. (Eds.): Geologie der Österreichischen Bundesländer. *Geologische Bundesanstalt,* Wien, 1–47.

Roetzel R. 2017: Bericht 2013–2016 über geologische Aufnahmen auf Blatt 21 Horn. *Jahrbuch Geol. Bundesanst.* 157, 317–328.

Roetzel R., Fuchs G., Batík P., Čtyroký P., Havlíček P. (Eds.) 2004: Geologische Karte der Nationalparks Thayatal und Podyjí 1:25,000. *Geologische Bundesanstalt*, Wien.

Rohais S., Eschard R. & Guillocheau F. 2008: Depositional model and stratigraphic architecture of rift climax Gilbert-type fan deltas (Gulf of Corinth, Greece). *Sediment. Geol.* 210, 132–145.

Ruffell A. & Worden R. 2000: Palaeoclimate analysis using spectral gamma-ray data from the Aptian (Cre ta ceous) of southern England and southern France. *Palaeogeogr. Palaeoclimatol. Palaeoecol.* 155, 265–283.

Schnyder J., Ruffell A., Deconinck J.-F. & Baudin F. 2006: Conjunctive use of spectral gamma-ray logs and clay mineralogy in defining late Jurassic–early Cretaceous palaeoclimate change (Dorset, U.K.). *Palaeogeogr. Palaeoclimatol. Palaeoecol.* 229, 303–320.

Schumm S.A. & Etheridge F.G. 1994: Origin, evolution and morphology of fluvial valleys. In: Dalrymple R.W., Boyd R. & Zaitlin B.A. (Eds.): Incised Valley Systems. Origin and Sedimentary Sequences. *Spec. Publ. Soc. Econ. Paleont. Miner.* 51, 11–27.

Schuster R. & Stüwe K. 2010: Die Geologie der Alpen im Zeitraffer. *Mitteilungen des naturwissenschaftlichen Vereins für Steiermark* 140, 5–21.

Shanley K.W. & McCabe P.J. 1994: Perspectives on the sequence stratigraphy of continental strata. *Am. Assoc. Petrol. Geol. Bull*. 78, 544–568.

Shpak P.F., Vishniakov I.B., Vul A.Y. & Ladyzhensky G.N. 1999: Geological structure peculiarities and oil and gas content of the Ukrainian Carpathian platform autochthon. *Biuletyn Państwowego Instytutu Geologicznego* 387, 175–181.

Sinclair H.D. 1997: Tectonostratigraphic model for underfilled peripheral foreland basin: An Alpine perspective. *Geol. Soc. Amer. Bull*. 109, 3, 324–346.

Triebold S., Eynatten H. von, Luvizotto G.L. & Zack T. 2007: Deducing source rock lithology from detrital rutile geochemistry: An example from the Erzgebirge, Germany. *Chem. Geol.* 244, 421–436.

Triebold S., von Eynatten H. & Zack T. 2012: A recipe for the use of rutile in sedimentary provenance analysis. *Sediment. Geol.* 282, 268–275.

Tucker M. (Ed.) 1995: Techniques in Sedimentology. *Blackwell Science*, Oxford, 1–394.

Viseras C., Calvache M.L., Soria J.M. & Fernandez J. 2003: Differential features of alluvial fans controlled by tectonic or eustatic accommodation space. Examples from the Betic Cordillera, Spain. *Geomorphology* 50, 181–202.

von Eynatten H. & Gaupp R. 1999: Provenance of Cretaceous synorogenic sandstones in the Eastern Alps: constraints from framework petrography, heavy mineral analysis and mineral chemistry. *Sediment. Geol.* 124, 81–111.

Walker R.G. & James N.P. 1992: Facies Models: Response to Sea Level Changes. *Geological Association of Canada*, St. John's, 1–317.

Waschbusch P.J. & Royden L.H. 1992: Spatial and temporal evolution of foredeep basins: lateral strength variations and inelastic yielding in continental lithoshere. *Basin Res.* 4, 179–196.

Weissmann G.S., Hartley A.J., Nichols, G.J., Scuderi L.A., Olsen M., Buehler H. & Banteah R.. 2010: Fluvial form in modern continental sedimentary basins: distributive fluvial systems. *Geology* 38, 39–42.

Went D.J. 2005: Pre-vegetation alluvial fan facies and processes: an example from the Cambro–Ordovician Rozel Conglomerate Formation, Jersey, Channel Islands. *Sedimentology* 52, 693–713.

Winter J. 1981: Exakte tephro-stratigraphische Korrelation mit morphologisch differenzierten Zironpopulationen (Grenzbereich Unter/Mitteldevon, Eifel-Ardennen). *Neues Jahrb. Geol. Paläontol., Abh.* 162, 1, 97–136.

Zack T., von Eynatten H. & Kronz A. 2004a: Rutile geochemistry and its potential use in quantitative provenance studies. *Sediment. Geol.* 171, 37–58.

Zack T., Moraes R. & Kronz A. 2004b: Temperature dependence of Zr in rutile: empirical calibration of a rutile thermometer. *Contrib. Mineral. Petrol.* 148, 471–488.

Zaitlin B.A., Dalrymple R.W. & Boyd R. 1994: The stratigraphic organization of incised-valley systems associated with relative sea-level change. In: Dalrymple R.W., Boyd R. & Zaitlin B.A. (Eds.): Incised Valley Systems. Origin and Sedimentary Sequences. *Spec. Publ. Soc. Econ. Paleont. Miner.* 51, 45–60.

Zimmerle W. 1979: Accessory Zircon from Rhyolite, Yellowstone National Park (Wyoming, U.S.A.). *Zeitschrift der Deutschen Geologischen Gesellschaft*. 130, 361–369.

Zingg T. 1935: Beitrag zur Schotteranalyse. Die Schotteranalyse und ihre Anwendung auf die Glattalschotter. *Schweizerische Mineralogische und Petrographische Mitteilungen* 15, 39–140.